Electronic Supplementary Material (ESI) for ChemComm.
This journal is © The Royal Society of Chemistry 2017

# Direct diversification of unmasked quinazolin-4(3*H*)-ones through orthogonal reactivity modulation

Jae Bin Lee, Mi Eun Kang, Joohee Kim, Chang Young Lee, Jung-Min Kee, Kyungjae Myung, Jang-Ung Park* and Sung You Hong*

**Supplementary Information**

## Table of Contents

## I. General Information

All reagents were purchased from standard suppliers (Sigma-Aldrich, Alfa Aesar, or TCI) and were used without further purification. All reactions were performed in oven-dried Schlenk tubes (capacity, 10 mL). $^{1}H$, $^{13}C$, and $^{19}F$ NMR spectra were recorded in DMSO-$d_6$ or $CDCl_3$ on a Bruker Avance III HD (400 MHz for proton, 100 MHz for carbon, 376 MHz for fluorine). All chemical shifts are given on the $\delta$-scale in ppm, and residual solvent peaks were used as references. High resolution mass spectrometry (HRMS) analyses were performed on a Thermo Scientific Q Exactive Plus Hybrid Quadrupole-Orbitrap mass spectrometer. Thin layer chromatography (TLC) was carried out on Merck Kieselgel 60 $F_{254}$ glass plates. Flash column chromatography was carried out using Merck Silica gel 60 silica.

## II. Substrate Synthesis and Characterization

Substrates **1a**–**1p**

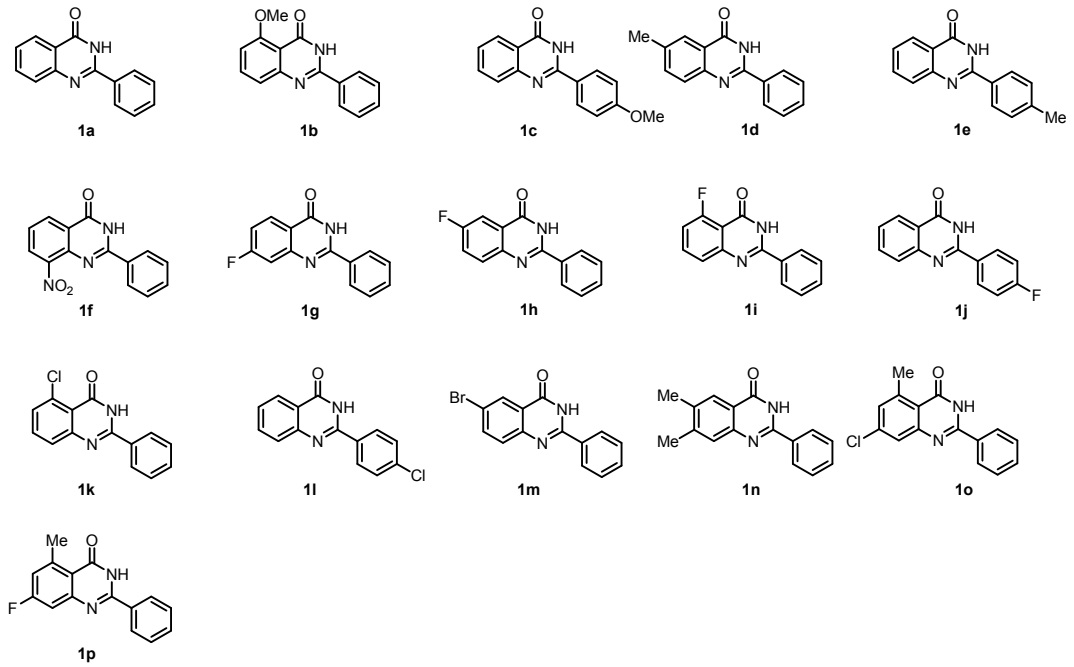


**General Procedure: Synthesis of 2-arylquinazolin-4(3*H*)-one (1a,1b,1d–1i,1k–1p)**

2-Arylquinazolin-4(3*H*)-ones were prepared according to the previously reported method.[S1] To a two-neck round bottom flask were added substituted 2-halobenzoic acid (8.55 mmol, 1.0 equiv) and benzamidine hydrochloride (12.77 mmol, 1.5 equiv) in DMF (20 mL). The reaction flask was evacuated, back-filled with nitrogen several times, and then vigorously stirred for 10 min. $Cs_2CO_3$ (17.03 mmol, 2.0 equiv) was added to the reaction mixture. After 15 min, CuI (1.70 mmol, 0.2 equiv) was subsequently added and stirred at room temperature for 12 h under a nitrogen atmosphere. After completion of the reaction, the reaction mixture was filtered. The solvent residue was concentrated *in vacuo* and the residue was purified by flash column chromatography.

**Procedure for the synthesis of 2-(4-methoxyphenyl)quinazolin-4(3*H*)-one (1c)**

2-(4-Methoxyphenyl)quinazolin-4(3*H*)-one was prepared according to the previously reported method.[S2] To a round bottom flask were added anthranilamide (20 mmol, 1.0 equiv), 4-methoxybenzaldehyde (20 mmol, 1.0 equiv) and $Cu_2O$ (0.6 mmol, 0.3 equiv) in DMA (60 mL), and stirred at 120 °C for 24 h under air. After completion of the reaction, the reaction mixture was filtered. The solvent residue was concentrated *in vacuo* and the residue was purified by flash column chromatography.

**Procedure for the synthesis of 2-(4-fluorophenyl)quinazolin-4(3*H*)-one (1j)**

2-(4-Fluorophenyl)quinazolin-4(3*H*)-one was prepared according to the previously reported method.[S3] To a round bottom flask were added anthranilamide (20 mmol, 1.0 equiv), 4-fluorobenzyl alcohol (20 mmol, 1.0 equiv), and KOH (40 mmol, 2.0 equiv) in toluene (80 mL), and stirred at 90 °C for 20 h under air. After completion of the reaction, the solvent residue was concentrated *in vacuo* and the residue was purified by flash column chromatography.

***1a**,[S1] **1b**,[S4] **1c**,[S2] **1d**,[S5] **1e**,[S5] **1g**,[S6] **1h**,[S5] **1i**,[S6] **1j**,[S3] **1k**,[S5] **1l**,[S5] and **1m**[S5] have been reported.

8-Nitro-2-phenylquinazolin-4(3*H*)-one (**1f**)

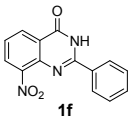

**1f**

Yellowish solid; **ATR-FTIR** ($cm^{-1}$): 3167, 3120, 3076, 1670, 1602, 1566, 1528, 1479, 1365, 1287, 1156, 1060, 966, 889, 825, 766, 692; **$^1$H NMR** (400 MHz, DMSO-$d_6$) δ 12.95 (s, 1H), 8.38 (d, *J* = 7.9, 1.4 Hz, 1H), 8.33 – 8.29 (m, 1H), 8.16 (d, *J* = 7.6 Hz, 2H), 7.68 – 7.54 (m, 4H); **$^{13}$C NMR** (100 MHz, DMSO-$d_6$) δ 161.38, 155.05, 147.10, 140.99, 132.64, 132.38, 130.15, 129.19, 129.00, 128.67, 128.59, 126.43, 122.97; **HRMS-ESI**: m/z $[M+H]^+$ calcd for $C_{14}H_{10}N_3O_3$: 268.0717; found: 268.0713.

6,7-Dimethyl-2-phenylquinazolin-4(3*H*)-one (**1n**)

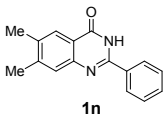

**1n**

White solid; **ATR-FTIR** ($cm^{-1}$): 3048, 2969, 2917, 1666, 1623, 1602, 1566, 1490, 1456, 1349, 1306, 1292, 1193, 1163, 1027, 998, 940, 851, 837, 776, 694; **$^1$H NMR** (400 MHz, DMSO-$d_6$) δ 12.36 (s, 1H), 8.15 (dt, *J* = 8.2, 1.8 Hz, 2H), 7.90 (s, 1H), 7.55 (dd, *J* = 5.2, 2.8 Hz, 4H), 2.39 (s, 3H), 2.37 (s, 3H); **$^{13}$C NMR** (100 MHz, DMSO-$d_6$) δ 162.49, 151.96, 147.65, 144.92, 136.32, 133.31, 131.63, 129.05, 128.03, 126.02, 119.21, 20.39, 19.77; **HRMS-ESI**: m/z $[M+H]^+$ calcd for $C_{16}H_{15}N_2O$: 251.1179; found: 251.1174.

7-Chloro-5-methyl-2-phenylquinazolin-4(3*H*)-one (**1o**)

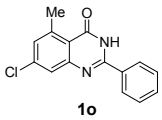

**1o**

White solid; **ATR-FTIR** ($cm^{-1}$): 3196, 3166, 3114, 2960, 2923, 2359, 1660, 1590, 1610, 1555, 1513, 1478, 1451, 1427, 1299, 1210, 1194, 1164, 1135, 1089, 1043, 986, 934, 890, 869, 849, 819, 777, 715, 693;**$^1$H NMR** (400 MHz, DMSO-$d_6$) δ 12.44 (s, 1H), 8.19 – 8.13 (m, 2H), 7.57 (dt, *J* = 15.9, 6.8 Hz, 4H), 7.35 (s, 1H), 2.80 (s, 3H); **$^{13}$C NMR** (100 MHz, DMSO-$d_6$) δ 162.92, 153.75, 151.87, 143.13, 138.37, 132.59, 132.12, 129.08, 128.89, 128.28, 125.08, 118.63, 22.68; **HRMS-ESI**: m/z $[M+H]^+$ calcd for $C_{15}H_{12}ClN_2O$: 271.0633; found: 271.0629.

7-Fluoro-5-methyl-2-phenylquinazolin-4(3*H*)-one (**1p**)

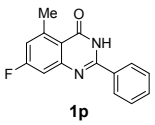

**1p**

White solid; **ATR-FTIR** ($cm^{-1}$): 3167, 3093, 3066, 2962, 2924, 2360, 2341, 1656, 1596, 1565, 1482, 1451, 1409, 1384, 1343, 1306, 1194, 1155, 1123, 1101, 1042, 1001, 979, 930, 862, 835, 780, 695;**$^1$H NMR** (400 MHz, DMSO-$d_6$) δ 12.40 (s, 1H), 8.21 – 8.12 (m, 2H), 7.62 – 7.51 (m, 3H), 7.31 (dd, *J* = 9.6, 2.5 Hz, 1H), 7.18 (d, *J* = 9.8 Hz, 1H), 2.82 (s, 3H); **$^{13}$C NMR** (100 MHz, DMSO-$d_6$) δ 164.91 (d, *J* = 250.4 Hz), 162.77, 153.63, 152.98 (d, *J* = 13.4 Hz), 144.51 (d, *J* = 10.8 Hz), 132.60, 132.08, 129.07, 128.27, 117.20 (d, *J* = 22.9 Hz), 116.87, 110.94 (d, *J* = 20.8 Hz), 23.07; **$^{19}$F NMR** (376 MHz, DMSO-$d_6$) δ -105.88; **HRMS-ESI**: m/z $[M+H]^+$ calcd for $C_{15}H_{12}FN_2O$: 255.0928; found: 255.0923.

# III. Products Synthesis and Characterization

## III.1 Optimization for the Synthesis of 3a

**Table S1** Initial catalyst screening[a]

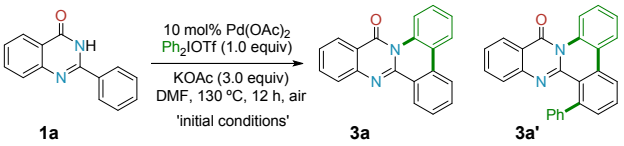


| Entry | Pd catalyst variations | Yield[b] (%) | |
|---|---|---|---|
| | | **3a** | **3a'** |
| 1 | -- | 37 | - |
| 2 | $(PPh_3)_2PdCl_2$ instead of $Pd(OAc)_2$ | - | - |
| 3 | PEPPSI-IPr instead of $Pd(OAc)_2$ | 13 | - |
| 4 | $Pd(TFA)_2$ instead of $Pd(OAc)_2$ | 17 | - |
| 5 | PEPPSI-SIPr instead of $Pd(OAc)_2$ | 28 | - |
| 6 | 30 mol% $Pd(OAc)_2$ instead of 10 mol% $Pd(OAc)_2$ | 49 | 0 |
| 7 | 40 mol% $Pd(OAc)_2$ instead of 10 mol% $Pd(OAc)_2$ | 73 | 3 |
| **8** | **50 mol% $Pd(OAc)_2$ instead of 10 mol% $Pd(OAc)_2$** | **82** | **5** |
| 9 | 70 mol% $Pd(OAc)_2$ instead of 10 mol% $Pd(OAc)_2$ | 77 | 8 |

[a] The initial conditions: **1a** (0.09 mmol, 1.0 equiv), $Ph_2IOTf$ (0.09 mmol, 1.0 equiv), $Pd(OAc)_2$ (10 mol%), KOAc (0.27 mmol, 3.0 equiv), DMF (2.0 mL), 130 °C, 12 h, air. [b] Yield determined by GC analysis using *n*-dodecane as an internal standard.

**Table S2** Base screening[a]

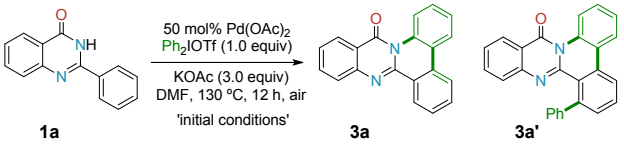


**1a** **3a** **3a'**

| Entry | Base variations | Yield[b] (%) | |
|---|---|---|---|
| | | **3a** | **3a'** |
| **1** | **--** | **82** | **5** |
| 2 | CsOAc instead of KOAc | 75 | 5 |
| 3 | NaOAc instead of KOAc | 68 | 8 |
| 4 | $K_2CO_3$ instead of KOAc | 67 | 20 |
| 5 | 2.0 equiv KOAc instead of 3.0 equiv KOAc | 70 | 6 |
| 6 | 2.5 equiv KOAc instead of 3.0 equiv KOAc | 74 | 4 |

[a] The initial conditions: **1a** (0.09 mmol, 1.0 equiv), $Ph_2IOTf$ (0.09 mmol, 1.0 equiv), $Pd(OAc)_2$ (50 mol%), KOAc (0.27 mmol, 3.0 equiv), DMF (2.0 mL), 130 °C, 12 h, air. [b] Yield determined by GC analysis using *n*-dodecane as an internal standard.

**Table S3** Solvent and temperature screening[a]

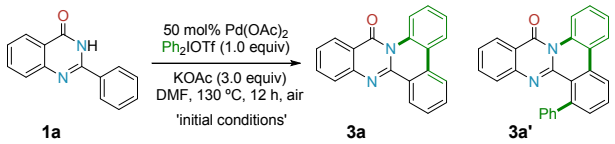


**1a** **3a** **3a'**

| Entry | Solvent and temperature variations | Yield[b] (%) | |
|---|---|---|---|
| | | **3a** | **3a'** |
| **1** | **--** | **82** | **5** |
| 2 | Toluene instead of DMF | 37 | 2 |
| 3 | DMSO instead of DMF | 72 | 2 |
| 4 | DMA instead of DMF | 82 | 6 |
| 5 | MeCN at 100 °C instead of DMF at 130 °C | 17 | - |
| 6 | DMC at 100 °C instead of DMF at 130 °C | 23 | 2 |
| 7 | THF at 100 °C instead of DMF at 130 °C | 20 | 1 |
| 8 | Dioxane at 100 °C instead of DMF at 130 °C | - | - |

[a] The initial conditions: **1a** (0.09 mmol, 1.0 equiv), $Ph_2IOTf$ (0.09 mmol, 1.0 equiv), $Pd(OAc)_2$ (50 mol%), KOAc (0.27 mmol, 3.0 equiv), DMF (2.0 mL), 130 °C, 12 h, air. [b] Yield determined by GC analysis using *n*-dodecane as an internal standard.

**Table S4** Oxidant screening[a]

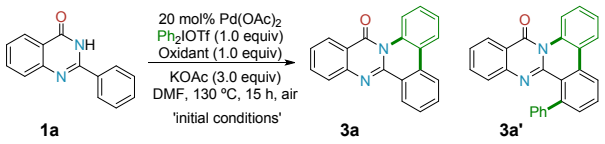


| Entry | Oxidant variations | Yield[b] (%) | |
|---|---|---|---|
| | | **3a** | **3a'** |
| 1[c] | -- | 82 | 5 |
| 2 | $Ag(OAc)_2$ | 31 | - |
| 3 | AgI | 17 | - |
| 4 | $AgCO_3$ | 12 | - |
| 5 | $AgNO_3$ | 10 | - |
| 6 | $Ag_2O$ | 38 | - |
| 7 | $AgSbF_6$ | 13 | - |
| **8** | **AgTFA** | **74** | **1** |

[a] The initial conditions: **1a** (0.09 mmol, 1.0 equiv), $Ph_2IOTf$ (0.09 mmol, 1.0 equiv), $Pd(OAc)_2$ (20 mol%), oxidant (0.09 mmol, 1.0 equiv), KOAc (0.27 mmol, 3.0 equiv), DMF (2.0 mL), 130 °C, 15 h, air. [b] Yield determined by GC analysis using *n*-dodecane as an internal standard. [c] 50 mol% $Pd(OAc)_2$ for 12 h instead of 20 mol% $Pd(OAc)_2$ for 15 h.

**Table S5** Ligand screening[a]

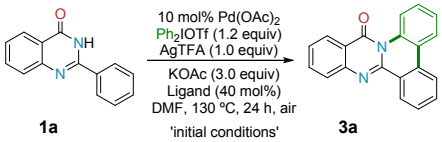


**1a** **3a**

| Entry | Ligand variations | Yield[b] (%) |
|---|---|---|
| 1[c] | -- | 74 |
| 2 | 2,2'-Bipyridyl | 2 |
| 3 | Bathophenanthroline | 1 |
| 4 | XPhos | 21 |
| 5 | *t*BuXPhos | 4 |
| 6 | XantPhos | 35 |
| 7 | CyJohnPhos | 43 |
| **8** | **BrettPhos** | **>99** |
| 9 | Tricyclohexylphosphine | 85 |
| 10 | Triphenylphosphine | 72 |

[a] The initial conditions: **1a** (0.09 mmol, 1.0 equiv), $Ph_2IOTf$ (0.11 mmol, 1.2 equiv), $Pd(OAc)_2$ (10 mol%), AgTFA (0.09 mmol, 1.0 equiv), ligand (40 mol%), KOAc (0.27 mmol, 3.0 equiv), DMF (2.0 mL), 130 °C, 24 h, air. [b] Yield determined by GC analysis using *n*-dodecane as an internal standard. [c] 20 mol% $Pd(OAc)_2$ and 1.0 equiv $Ph_2IOTf$ are used for 15 h.

**Table S6** Selected optimization conditions under an oxygen atmosphere[a]

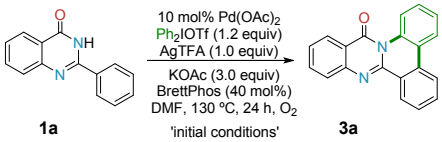


**1a** **3a**

| Entry | Reaction conditions | Yield[b] (%) |
|---|---|---|
| 1 | **-** | **76** |
| 2 | 20 mol% $Pd(OAc)_2$ | 78 |
| 3 | 20 mol% BrettPhos | 63 |
| **4** | **20 mol% $Pd(OAc)_2$, 30 mol% BrettPhos, 1.1 equiv $Ph_2IOTf$ and 4.0 equiv KOAc** | **97** |

[a] The initial conditions: **1a** (0.09 mmol, 1.0 equiv), $Ph_2IOTf$ (0.11 mmol, 1.2 equiv), $Pd(OAc)_2$ (10 mol%), BrettPhos (40 mol%), AgTFA (0.09 mmol, 1.0 equiv), KOAc (0.27 mmol, 3.0 equiv), DMF (2.0 mL), 130 °C, 24 h, $O_2$. [b] Isoated yield.

### III.2 Procedure for the *N*-arylation (2a)

To a Schlenk tube were added 2-phenylquinazolin-4(3*H*)-one **1a** (0.09 mmol, 1.0 equiv), $Ph_2IOTf$ (0.135 mmol, 1.5 equiv), CuI (0.009 mmol, 10 mol%), $Na_2CO_3$ (0.18 mmol, 2.0 equiv), Li-*t*-Yu-butyl-quinoline **L7** (0.036, 40 mol%) and DMF (2.0 mL). The resulting mixture was stirred at 130 °C for 24 h. The reaction was monitored by TLC or GC analysis. After completion of the reaction, the reaction mixture was concentrated *in vacuo* and purified by flash column chromatohraphy.

***2a**[S7] has been reported.

### III.3 Procedure for the Annuative π-Extension (3)

To a Schlenk tube were added 2-arylquinazolin-4(3*H*)-one **1** (0.09 mmol, 1.0 equiv), $Ar_2IOTf$ (0.10 mmol, 1.1 equiv), $Pd(OAc)_2$ (0.018 mmol, 20 mol%), BrettPhos (0.027 mmol, 30 mol%), KOAc (0.36 mmol, 4.0 equiv), AgTFA (0.09 mmol, 1.0 equiv) and DMF (2.0 mL). The resulting mixture was bubbled with oxygen for 5 min, and then stirred at 130 °C for 24 h under an $O_2$ atmosphere. The reaction was monitored by TLC or GC analysis. After completion of the reaction, the reaction mixture was concentrated *in vacuo* and purified by flash column chromatohraphy.

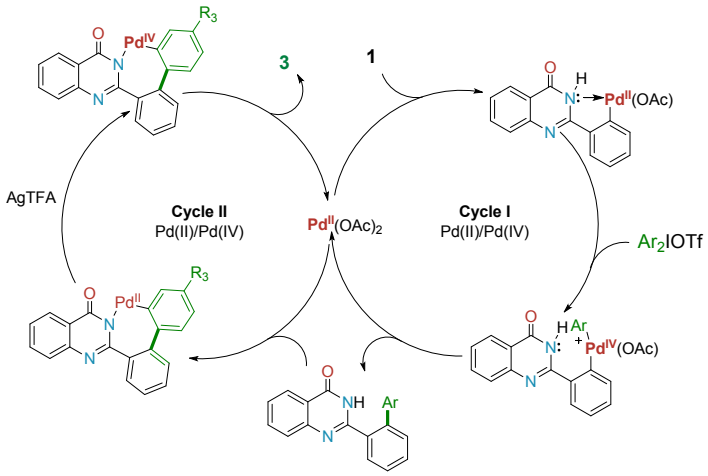


**Scheme S1** Proposed mechanism of annulative π-extension: alternative Pd(II)/Pd(IV) manifold in cycle II.

***3a**,[S8] **3c**,[S8] **3d**,[S9] **3e**,[S8] **3h**,[S9] **3j**,[S8] **3l**,[S8] **3q**,[S10] **3r**,[S10] and **3s**[S10] have been reported.

13-Methoxy-14*H*-quinazolino[3,2-*f*]phenanthridin-14-one (**3b**)

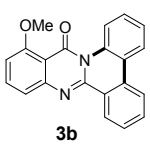
**3b**

White solid (92%); **ATR-FTIR** ($cm^{-1}$): 3009, 2922, 2852, 2239, 1683, 1593, 1547, 1470, 1346, 1261, 1101, 1085, 1024, 914, 860, 810, 779, 747, 717; **$^1$H NMR** (400 MHz, $CDCl_3$) δ 8.95 (dd, *J* = 8.1, 1.4 Hz, 1H), 8.91 – 8.86 (m, 1H), 8.26 – 8.17 (m, 2H), 7.70 (td, *J* = 8.2, 7.6, 6.3 Hz, 2H), 7.58 (ddd, *J* = 8.2, 7.1, 1.2 Hz, 1H), 7.45 (tdt, *J* = 8.2, 5.6, 2.9 Hz, 2H), 7.41 – 7.36 (m, 1H), 6.91 (dd, *J* = 8.3, 0.9 Hz, 1H), 4.07 (s, 3H); **$^{13}$C NMR** (100 MHz, $CDCl_3$) δ 160.11, 159.09, 147.71, 145.71, 133.74, 131.68, 131.18, 130.54, 127.41, 126.99, 126.92, 125.91, 125.13, 121.98, 121.93, 121.03, 120.74, 118.07, 109.67, 106.13, 55.38; **HRMS-ESI**: m/z $[M+H]^+$ calcd for $C_{21}H_{15}N_2O_2$: 327.1128; found: 327.1123.

10-Nitro-14*H*-quinazolino[3,2-*f*]phenanthridin-14-one (**3f**)

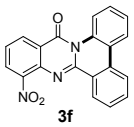
**3f**

Yellowish solid (89%); **ATR-FTIR** ($cm^{-1}$): 3081, 2959, 2923, 2854, 1732, 1693, 1597, 1550, 1523, 1447, 1362, 1335, 1258, 11522, 1018, 869, 799, 760, 738, 714; **$^{1}$H NMR** (400 MHz, $CDCl_3$) δ 9.11 – 9.06 (m, 1H), 9.02 (dd, *J* = 8.2, 1.4 Hz, 1H), 8.65 (dd, *J* = 8.1, 1.5 Hz, 1H), 8.36 – 8.22 (m, 3H), 7.81 (ddd, *J* = 8.3, 7.1, 1.5 Hz, 1H), 7.65 (ddd, *J* = 8.2, 7.2, 1.2 Hz, 1H), 7.60 – 7.52 (m, 3H); **$^{13}$C NMR** (100 MHz, $CDCl_3$) δ 160.39, 147.52, 144.56, 138.05, 132.33, 131.33, 131.09, 130.76, 128.27, 128.05, 127.77, 127.41, 126.18, 125.46, 123.70, 122.27, 122.23, 121.32, 121.11, 120.77; **HRMS-ESI**: m/z $[M+H]^+$ calcd for $C_{20}H_{12}N_3O_3$: 342.0873; found: 342.0868.

11-Fluoro-14*H*-quinazolino[3,2-*f*]phenanthridin-14-one (**3g**)

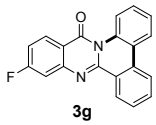
**3g**

White solid (91%); **ATR-FTIR** ($cm^{-1}$): 2922, 2852, 1686, 1597, 1552, 1474, 1451, 1335, 1281, 1149, 1089, 1041, 971, 858, 774, 764, 746, 715; **$^{1}$H NMR** (400 MHz, $CDCl_3$) δ 9.08 (dd, *J* = 8.0, 1.8 Hz, 1H), 8.97 (dd, *J* = 8.1, 1.3 Hz, 1H), 8.41 (dd, *J* = 8.9, 6.1 Hz, 1H), 8.31 – 8.18 (m, 3H), 7.80 – 7.70 (m, 1H), 7.67 – 7.57 (m, 1H), 7.56 – 7.46 (m, 2H), 7.21 (td, *J* = 8.5, 2.5 Hz, 1H); **$^{13}$C NMR** (100 MHz, $CDCl_3$) δ 166.74 (d, *J* = 254.4 Hz), 162.22, 148.22 (d, *J* = 13.5 Hz), 147.54, 132.86, 132.52, 131.51, 130.22 (d, *J* = 10.8 Hz), 128.60, 128.35, 128.20, 126.83, 126.59, 123.09, 123.02, 122.17, 121.81, 117.50, 115.10 (d, *J* = 23.7 Hz), 111.90 (d, *J* = 21.7 Hz); **$^{19}$F NMR** (376 MHz, $CDCl_3$) δ -103.10; **HRMS-ESI**: m/z $[M+H]^+$ calcd for $C_{20}H_{12}FN_2O$: 315.0928; found: 315.0926.

13-Fluoro-14*H*-quinazolino[3,2-*f*]phenanthridin-14-one (**3i**)

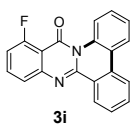
**3i**

White solid (64%); **ATR-FTIR** ($cm^{-1}$): 3076, 2926, 2853, 2360, 1674, 1603, 1553, 1482, 1453, 1359, 1291, 1242, 1152, 1108, 947, 833, 782, 743, 714; **$^{1}$H NMR** (400 MHz, $CDCl_3$) δ 8.97 – 8.89 (m, 2H), 8.21 (dd, *J* = 9.9, 7.7 Hz, 2H), 7.77 – 7.68 (m, 2H), 7.58 (dt, *J* = 7.6, 3.5 Hz, 2H), 7.48 (ddd, *J* = 6.8, 4.5, 1.8 Hz, 2H), 7.12 (dd, *J* = 10.7, 8.1 Hz, 1H); **$^{13}$C NMR** (100 MHz, $CDCl_3$) δ 161.38 (d, *J* = 266.2 Hz), 148.19, 147.15, 134.74 (d, *J* = 10.7 Hz), 132.52, 132.43, 131.56, 131.26, 128.55, 128.21, 128.16, 128.12, 127.55, 126.66, 126.58, 123.09, 122.96, 122.76 (d, *J* = 4.2 Hz), 121.89 (d, *J* = 14.6 Hz), 112.45 (d, *J* = 21.0 Hz); **$^{19}$F NMR** (376 MHz, $CDCl_3$) δ -111.48; **HRMS-ESI**: m/z $[M+H]^+$ calcd for $C_{20}H_{12}FN_2O$: 315.0928; found: 315.0925.

13-Chloro-14*H*-quinazolino[3,2-*f*]phenanthridin-14-one (**3k**)

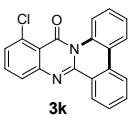
**3k**

Yellowish solid (66%); **ATR-FTIR** ($cm^{-1}$): 3062, 2957, 2920, 2851, 1736, 1691, 1571, 1540, 1452, 1342, 1238, 1148, 1118, 1017, 965, 896, 862, 809, 769, 748, 718; **$^{1}$H NMR** (400 MHz, $CDCl_3$) δ 8.97 (dd, *J* = 8.1, 1.4 Hz, 1H), 8.86 – 8.80 (m, 1H), 8.26 (ddd, *J* = 7.7, 5.0, 2.0 Hz, 2H), 7.79 – 7.71 (m, 2H), 7.68 – 7.60 (m, 2H), 7.55 – 7.48 (m, 3H); **$^{13}$C NMR** (100 MHz, $CDCl_3$) δ 160.11, 147.64, 145.88, 133.56, 133.03, 132.78, 131.56, 131.40, 130.61, 127.61, 127.57, 127.19, 127.06, 125.58, 125.07, 122.14, 122.01, 120.88, 120.81, 116.93; **HRMS-ESI**: m/z $[M+H]^+$ calcd for $C_{20}H_{12}ClN_2O$: 331.0633; found: 331.0628.

12-Bromo-14*H*-quinazolino[3,2-*f*]phenanthridin-14-one (**3m**)

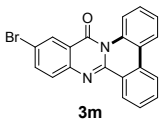
**3m**

Yellowish solid (78%); **ATR-FTIR** ($cm^{-1}$): 2921, 2852, 1734, 1679, 1599, 1552, 1469, 1449, 1341, 1288, 1259, 1147, 1093, 1017, 881, 761, 742, 714; **$^1$H NMR** (400 MHz, $CDCl_3$) δ 9.11 (dd, *J* = 8.1, 1.7 Hz, 1H), 9.03 (dt, *J* = 8.2, 0.9 Hz, 1H), 8.43 (dd, *J* = 8.0, 1.1 Hz, 1H), 8.30 – 8.21 (m, 1H), 7.85 – 7.82 (m, 2H), 7.79 – 7.71 (m, 1H), 7.66 – 7.59 (m, 1H), 7.51 (ddd, *J* = 9.2, 6.0, 2.0 Hz, 3H); **$^{13}$C NMR** (100 MHz, $CDCl_3$) δ 162.99, 146.14, 134.55, 133.51, 133.08, 132.22, 131.35, 128.98, 128.56, 128.24, 128.14, 127.41, 127.17, 126.94, 126.49, 126.25, 123.12, 123.10, 122.18, 121.82; **HRMS-ESI**: m/z $[M+H]^+$ calcd for $C_{20}H_{12}BrN_2O$: 375.0128; found: 375.0128.

11,12-Dimethyl-14*H*-quinazolino[3,2-*f*]phenanthridin-14-one (**3n**)

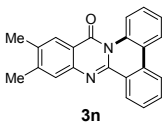
**3n**

White solid (98%); **ATR-FTIR** ($cm^{-1}$): 2961, 2920, 2852, 2593, 2226, 1950, 1730, 1677, 1598, 1551, 1473, 1432, 1326, 1286, 1259, 1148, 1088, 1020, 870, 799, 766, 746, 716; **$^1$H NMR** (400 MHz, $CDCl_3$) δ 9.11 (dd, *J* = 7.5, 1.2 Hz, 1H), 8.98 (ddd, *J* = 8.1, 1.5, 0.5 Hz, 1H), 8.26 – 8.20 (m, 2H), 8.16 (d, *J* = 1.0 Hz, 1H), 7.75 – 7.69 (m, 1H), 7.62 – 7.56 (m, 2H), 7.54 – 7.44 (m, 2H), 2.46 (s, 3H), 2.45 (s, 3H); **$^{13}$C NMR** (100 MHz, $CDCl_3$) δ 161.88, 144.91, 143.95, 143.56, 134.99, 132.25, 130.89, 130.16, 127.46, 127.03, 127.01, 126.45, 126.07, 125.27, 122.08, 122.03, 121.20, 120.97, 120.76, 117.67, 19.50, 18.83; **HRMS-ESI**: m/z $[M+H]^+$ calcd for $C_{22}H_{17}N_2O$: 325.1335; found: 325.1332.

11-Chloro-13-methyl-14*H*-quinazolino[3,2-*f*]phenanthridin-14-one (**3o**)

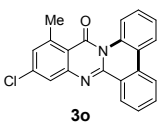
**3o**

White solid (83%); **ATR-FTIR** ($cm^{-1}$): 3084, 2969, 2924, 1691, 1586,1573, 1547, 1443, 1341, 1322, 1281, 1149, 1029, 896, 857, 753, 744, 719; **$^1$H NMR** (400 MHz, $CDCl_3$) δ 8.91 (dd, *J* = 8.1, 1.4 Hz, 1H), 8.84 – 8.79 (m, 1H), 8.28 – 8.18 (m, 2H), 7.73 (ddd, *J* = 8.2, 7.1, 1.4 Hz, 1H), 7.64 – 7.56 (m, 2H), 7.53 – 7.43 (m, 2H), 7.21 (dq, *J* = 1.8, 0.9 Hz, 1H), 2.92 (s, 3H); **$^{13}$C NMR** (100 MHz, $CDCl_3$) δ 161.89, 147.56, 146.03, 142.00, 138.40, 131.53, 131.40, 130.51, 127.74, 127.55, 127.04, 126.98, 125.73, 125.39, 123.40, 122.15, 122.06, 120.78, 120.74, 116.81, 21.98; **HRMS-ESI**: m/z $[M+H]^+$ calcd for $C_{21}H_{14}ClN_2O$: 345.0789; found: 345.0782.

11-Fluoro-13-methyl-14*H*-quinazolino[3,2-*f*]phenanthridin-14-one (**3p**)

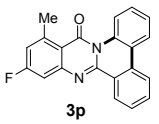
**3p**

White solid (99%); **ATR-FTIR** ($cm^{-1}$): 3077, 2960, 2926, 2852, 1734, 1694, 1594, 1555, 1451, 1333, 1290, 1258, 1143, 1113, 1030, 1004, 986, 855, 766, 715; **$^1$H NMR** (400 MHz, $CDCl_3$) δ 8.94 (ddd, *J* = 8.1, 1.5, 0.5 Hz, 1H), 8.87 – 8.80 (m, 1H), 8.28 – 8.20 (m, 2H), 7.74 (ddd, *J* = 8.2, 7.2, 1.5 Hz, 1H), 7.60 (ddd, *J* = 8.2, 7.2, 1.2 Hz, 1H), 7.53 – 7.44 (m, 2H), 7.31 – 7.27 (m, 1H), 6.99 (ddq, *J* = 9.5, 2.6, 0.9 Hz, 1H), 2.95 (s, 3H); **$^{13}$C NMR** (100 MHz, $CDCl_3$) δ 164.37 (d, *J* = 253.5 Hz), 161.75, 148.93, 148.79, 146.03, 143.72 (d, *J* = 10.6 Hz), 131.57, 131.40, 130.56, 127.55, 127.02 (d, *J* = 8.0 Hz), 125.72, 125.33, 122.15, 122.05, 120.80, 116.04 (d, *J* = 23.0 Hz), 115.22, 115.20, 109.00 (d, *J* = 21.1 Hz), 22.38 (d, *J* = 1.5 Hz); **$^{19}$F NMR** (376 MHz, $CDCl_3$) δ -104.72; **HRMS-ESI**: m/z $[M+H]^+$ calcd for $C_{21}H_{14}FN_2O$: 329.1085; found: 329.1081.

### III.4 Procedure for the C–H Fluorination (4a)

To a Schlenk tube were added 2-phenylquinazolin-4(3*H*)-one **1a** (0.09 mmol, 1.0 equiv), $Pd(OAc)_2$ (10 mol%), NFSI (0.27 mmol, 3.0 equiv) and DMF (2.0 mL). The resulting mixture was stirred at 150 °C for 12 h. The reaction was monitored by TLC or GC analysis. After the completion of the reaction, the reaction mixture was concentrated *in vacuo*, and purified by flash column chromatohraphy.

***4a**[S11] has been reported.

## IV. Detection of $Hg^{2+}$ Using FET Sensors

### IV.1 Methods

#### Fabrication of Chemically-Modified Graphene FET

Photoresist was patterned on Si substrates with 300 nm thick $SiO_2$, and Cr/Au (3 nm/100 nm) electrodes were made by thermal evaporation. Then, graphene was transferred onto the Cr/Au electrodes and patterned by photolithography. Graphene film was dry-etched using oxygen reactive ion etching (RIE) plasma for channel. Graphene channel was surface modified by dip coating of **3a** (300 ppm) in MeOH/DCM (9:1, v/v) via the π-π stacking interaction.

#### Fabrication of Graphene-AgNW Hybrid Field-Effect Sensors and Integration with μ-Fluidic Channel

For making the μ-fluidic channel, SU-8 3050 negative photoresist was spin coated onto a bare Si wafer, followed by patterning by photolithography process. A mixture of Sylgard 184 silicone elastomer and curing agent (10:1 wt.%) was poured onto the Si wafer with the thickness of 5 mm and cured at 60 °C for 5 h. The cured PDMS was peeled from the master, and then input, output, and gate terminals were punched out of the PDMS with steel tubes. The Ag/AgCl reference electrode was inserted into the PDMS channel through the gate terminal.

#### Real-time Sensing of $Hg^{2+}$ by Chemically-Modified Graphene-FET

The flow rate of all solutions in the μ-fluidic channel was 1.0 mL $h^{-1}$. For the real-time sensing, $Hg(CN)_2$ solution (100 ppm) and imidazole solution (aqueous, 20 mM) were consecutively injected in the μ-fluidic channel. A solution-gate characterization was conducted by sweeping Ag/AgCl reference electrode using a probe station (Keithley 4200-SCS semiconductor parametric analyzer). All devices were characterized at 0.1 V of drain bias.

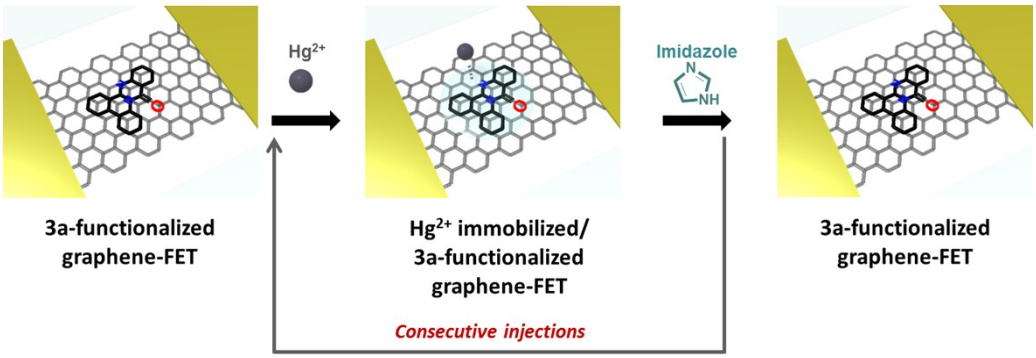


**Scheme S2** Reversible and real-time sensing of $Hg^{2+}$ using chemically-modified graphene-FET.

### IV.2 Electronic Characteristics of FET for Other Metal Ions

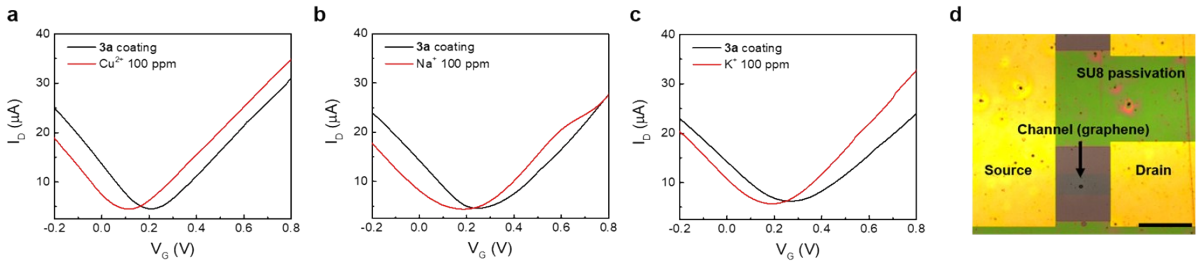


**Fig. S1** Transfer characteristics of solution-gated graphene field-effect sensors with **3a-**functionalization after flowing (a) $Cu^{2+}$ solution, (b) $Na^{+}$ solution, (c) $K^{+}$ solution ($V_D$ = 0.1 V). (d) Optical microscope image of fabricated graphene field-effect sensor. Scale bar, 500 μm. Concentration the solution: $Cu(OAc)_2$, NaCl, or KCl; 100 ppm.

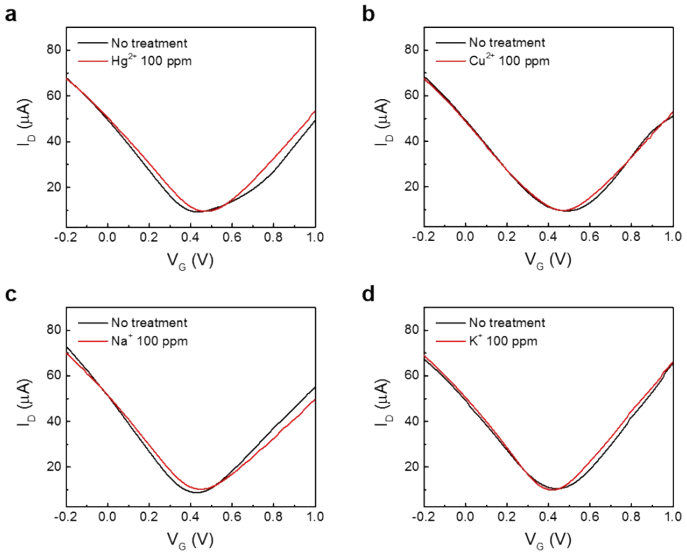


**Fig. S2** Transfer characteristics of solution-gated graphene field-effect sensors without **3a-**functionalization after flowing (a) $Hg^{2+}$ solution, (b) $Cu^{2+}$ solution, (c) $Na^{+}$ solution, (d) $K^{+}$ solution ($V_D$ = 0.1 V).

## V. References


S1 X. Liu, H. Fu, Y. Jiang and Y. Zhao, *Angew. Chem., Int. Ed.,* 2009, **48**, 348.

S2 D. Zhan, T. Li, H. Wei, W. Weng, K. Ghandi and Q. Zheng, *RSC Adv.*, 2012, **3**, 9325.

S3 D. Qui, Y. Wang, D. Lu, L. Zhou and Q. Zeng, *Monatsh. Chem.*, 2015, **146**, 1343.

S4 M. Hayakawa, H. Kaizawa, H. Moritomo, T. Koizumi, T. Ohishi, M. Okada, M. Ohta, S.-i. Tsukamoto, P. Parker, P. Workman and M. Waterfield, *Bioorg. Med. Chem.,* 2006, **14**, 6847.

S5 F. -C. Jia, Z. -W. Zhou, C. Xu, Y. -D. Wu and A. -X. Wu, *Org. Lett.,* 2016, **18**, 2942.

S6 F. Li, L. Lu and J. Ma, *Org. Chem. Front.,* 2015, **2**, 1589.

S7 T. Kotipalli, V. Kavala, D. Janreddy, V. Bandi, C.-W. Kuo and C.-F. Yao, *Eur. J. Org. Chem.* 2016, **2016**, 1182.

S8 P. K. Gupta, N. Yadav, S. Jaiswal, M. Asad, R. Kant and K. Hajela, *Chem. Eur. J.,* 2015, **21**, 13210.

S9 Y. Yu, Y. Yue, D. Wang, X. Li and C. Chen and J. Peng, *Synthesis,* 2016, **48**, 3941.

S10 B. Banerji, S. Bera, S. Chatterjee, S. K. Killi and S. Adhikary, *Chem. Eur. J.,* 2016, **22**, 3506.

S11 R. Sharma, R. A. Vishwakarma and S. B. Bharate, *Eur. J. Org. Chem.,* 2016, **2016**, 5227.

## VI. NMR Spectra

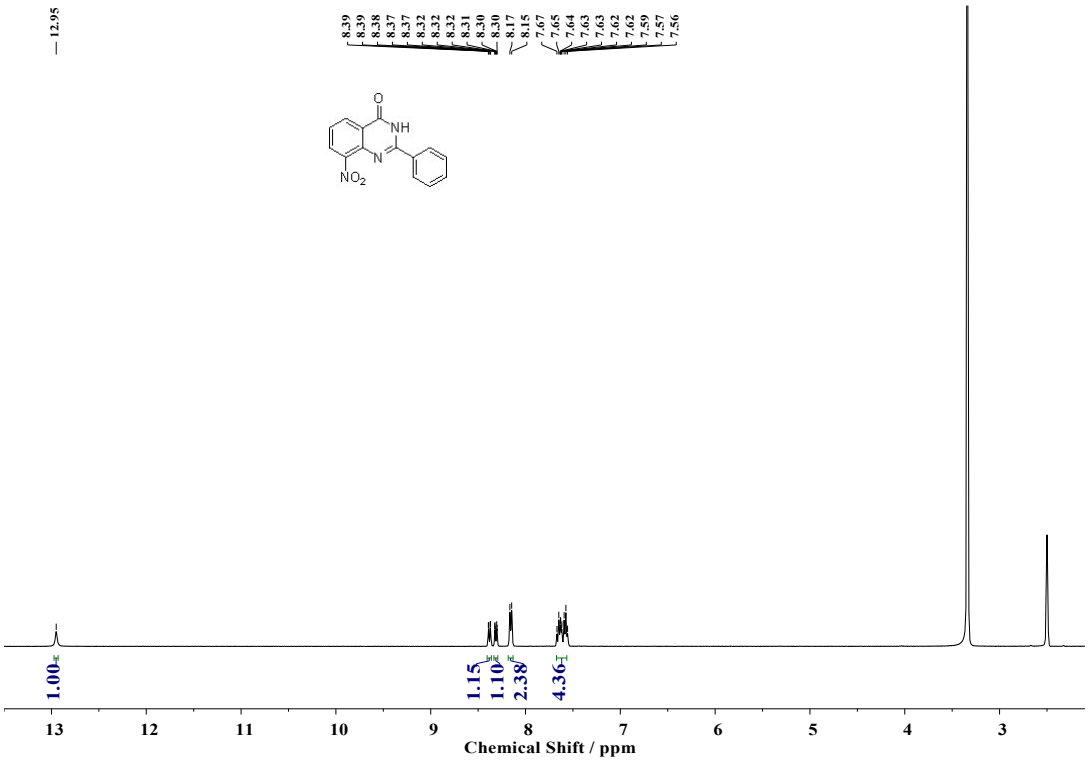


**Fig. S3** $^{1}$H NMR (400 MHz, DMSO-$d_6$) of the compound **1f**.

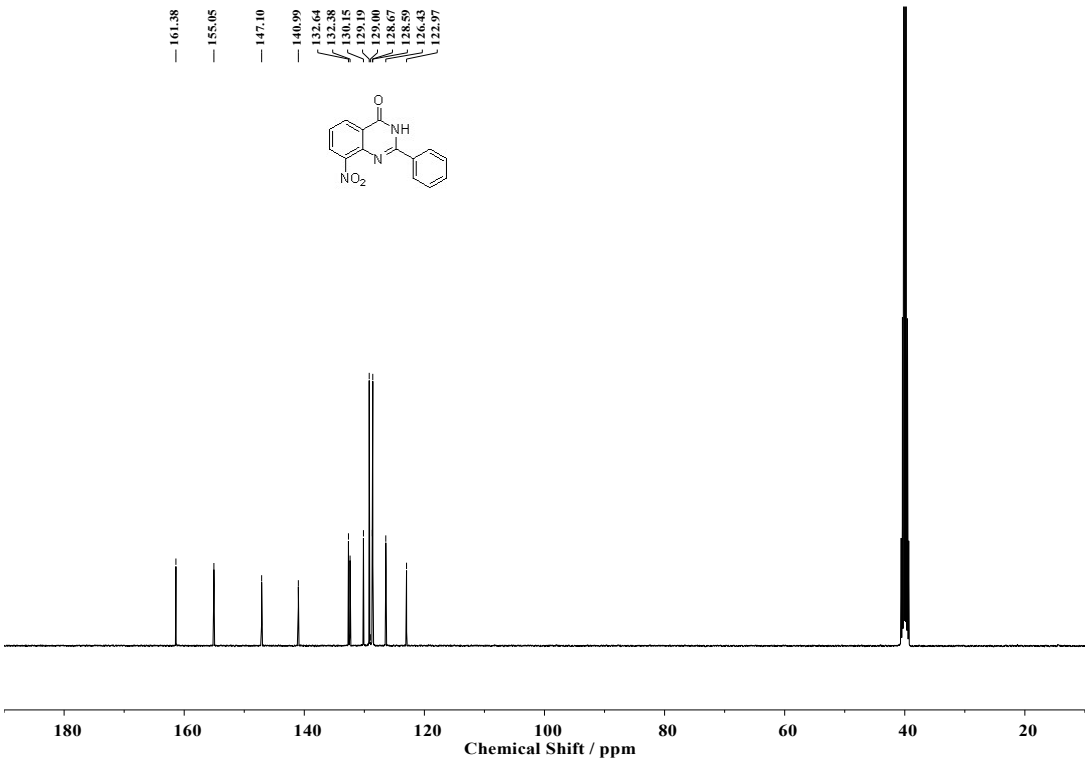


**Fig. S4** $^{13}$C NMR (100 MHz, DMSO-$d_6$) of the compound **1f**.

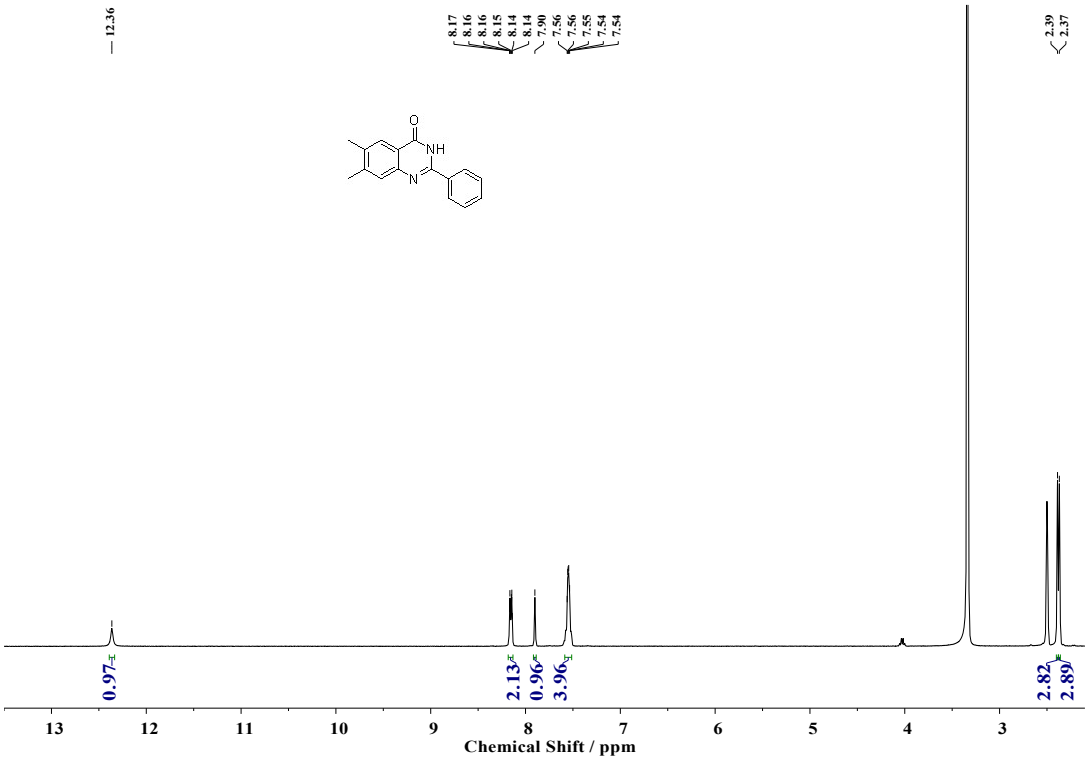


**Fig. S5** $^{1}$H NMR (400 MHz, DMSO-$d_6$) of the compound **1n**.

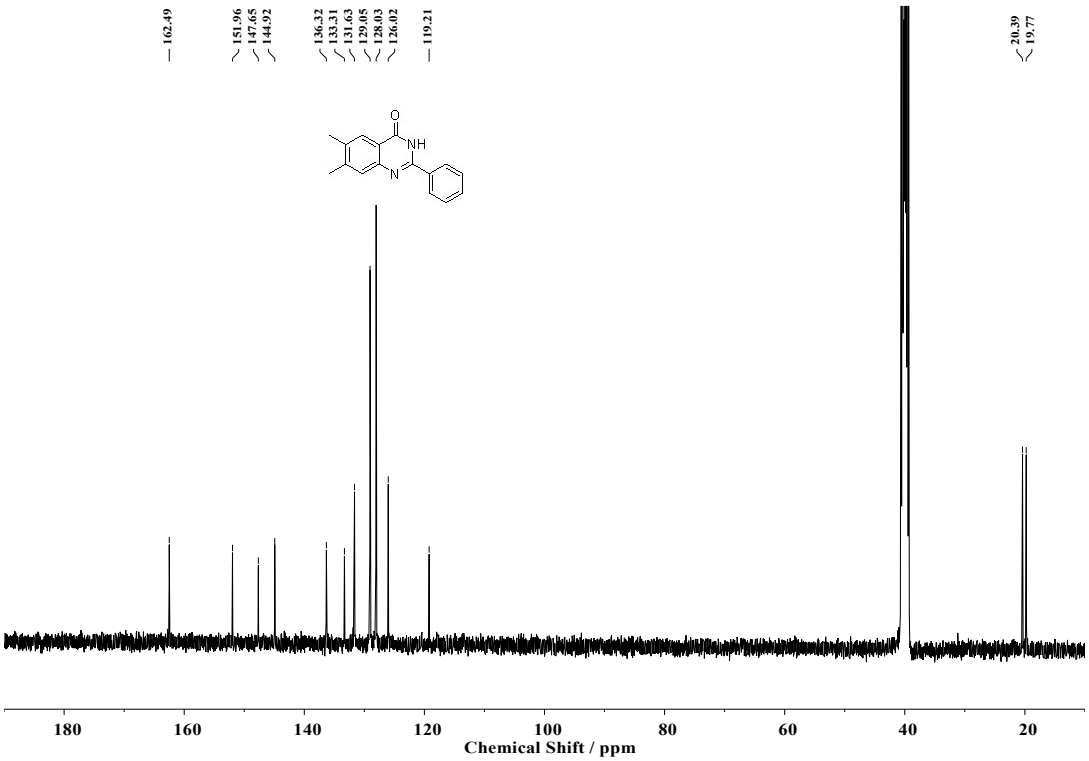


**Fig. S6** $^{13}$C NMR (100 MHz, DMSO-$d_6$) of the compound **1n**.

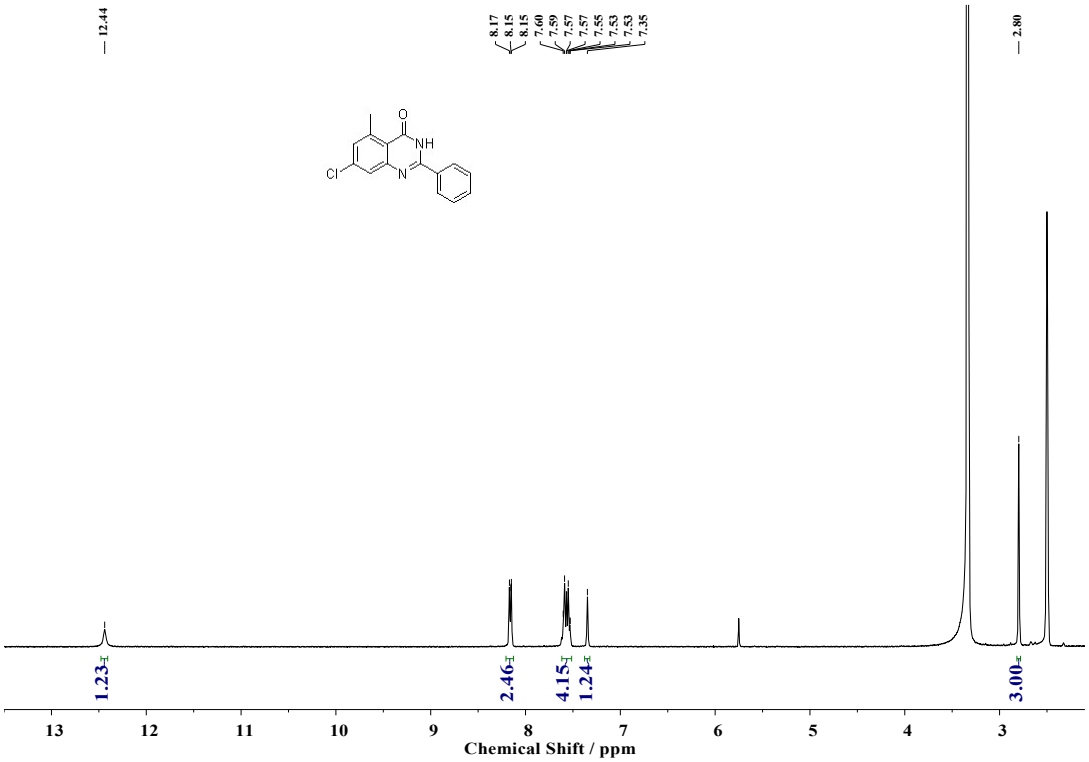


**Fig. S7** $^{1}$H NMR (400 MHz, DMSO-$d_6$) of the compound **1o**.

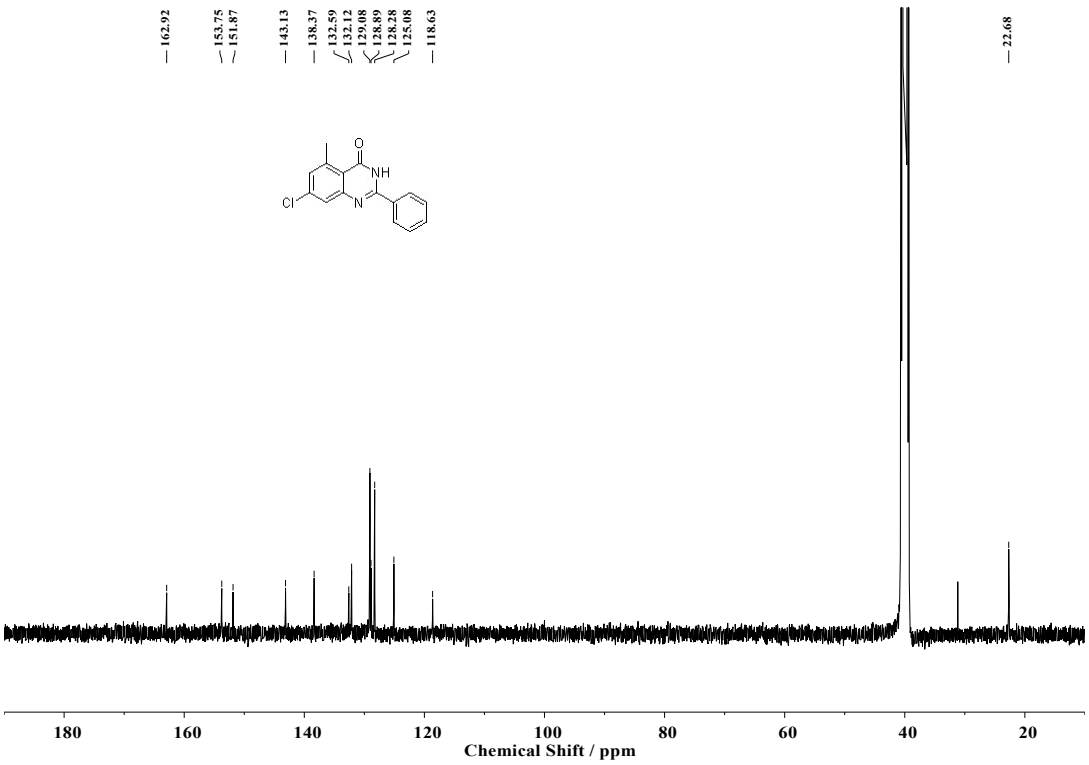


**Fig. S8** $^{13}$C NMR (100 MHz, DMSO-$d_6$) of the compound **1o**.

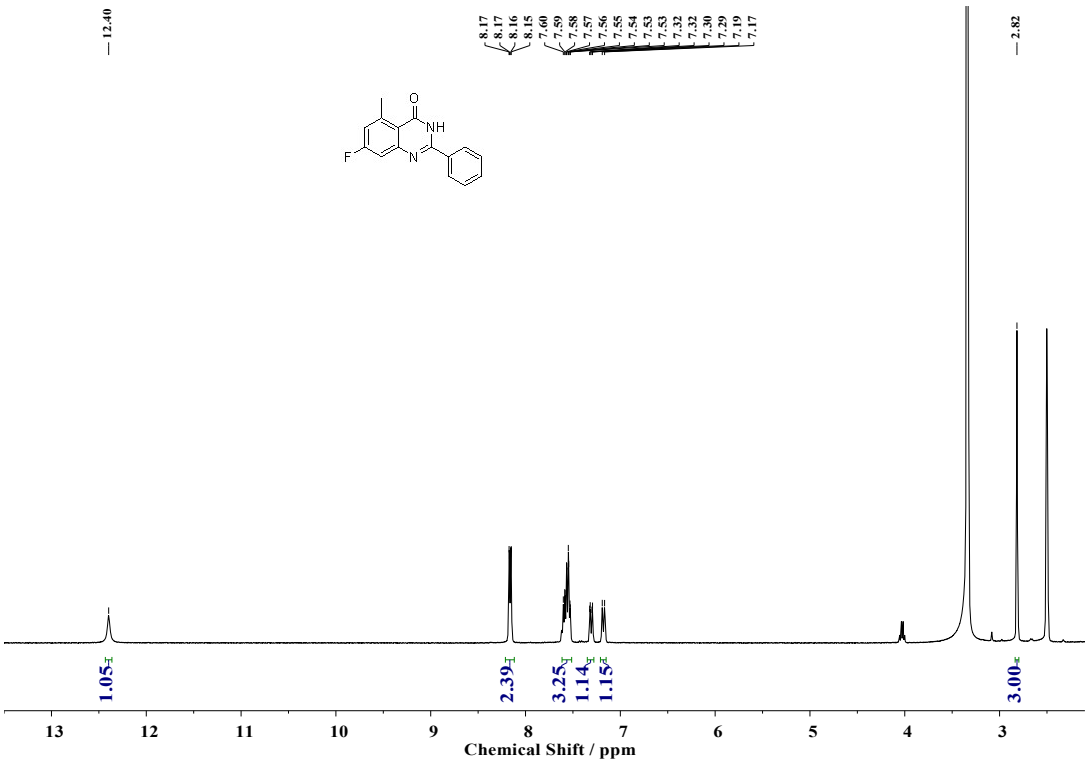


**Fig. S9** $^{1}$H NMR (400 MHz, DMSO-$d_6$) of the compound **1p**.

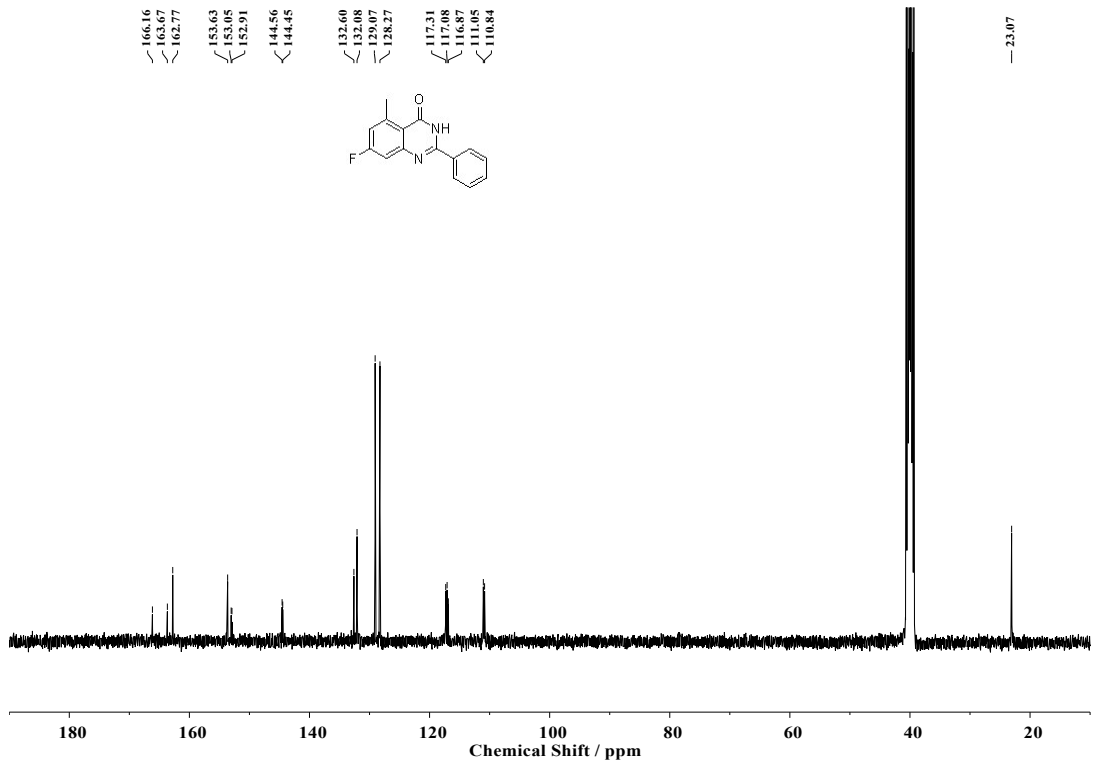


**Fig. S10** $^{13}$C NMR (100 MHz, DMSO-$d_6$) of the compound **1p**.

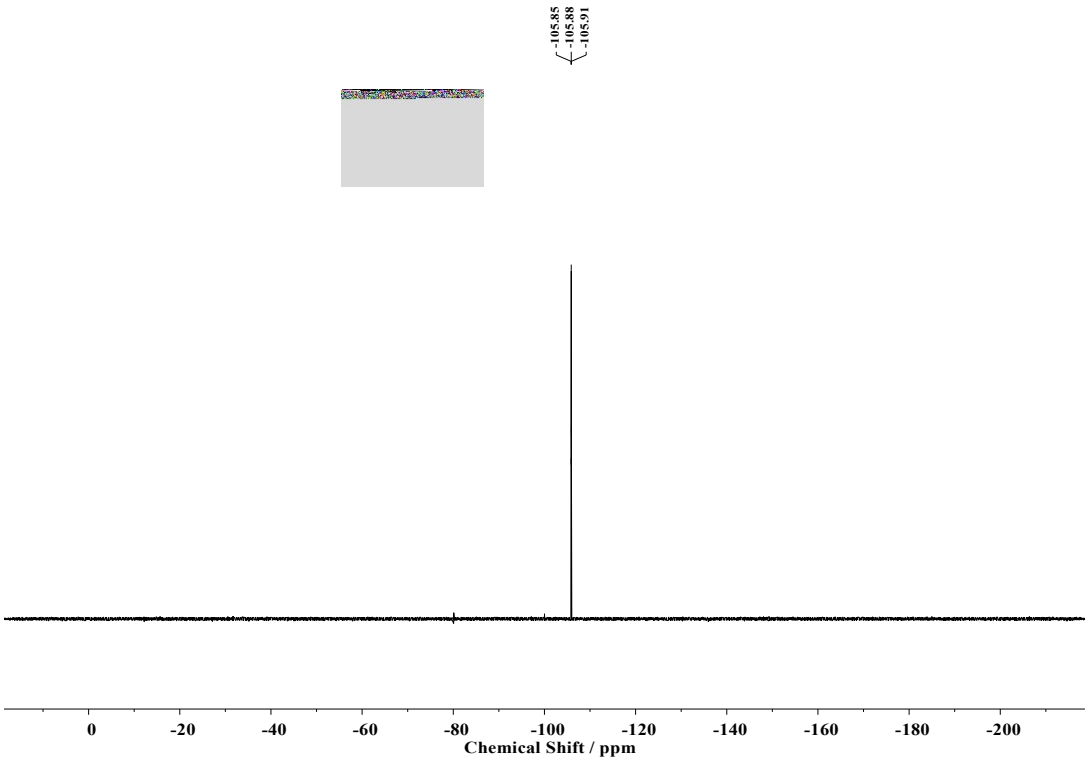


**Fig. S11** $^{13}F$ NMR (376 MHz, DMSO-$d_6$) of the compound **1p**.

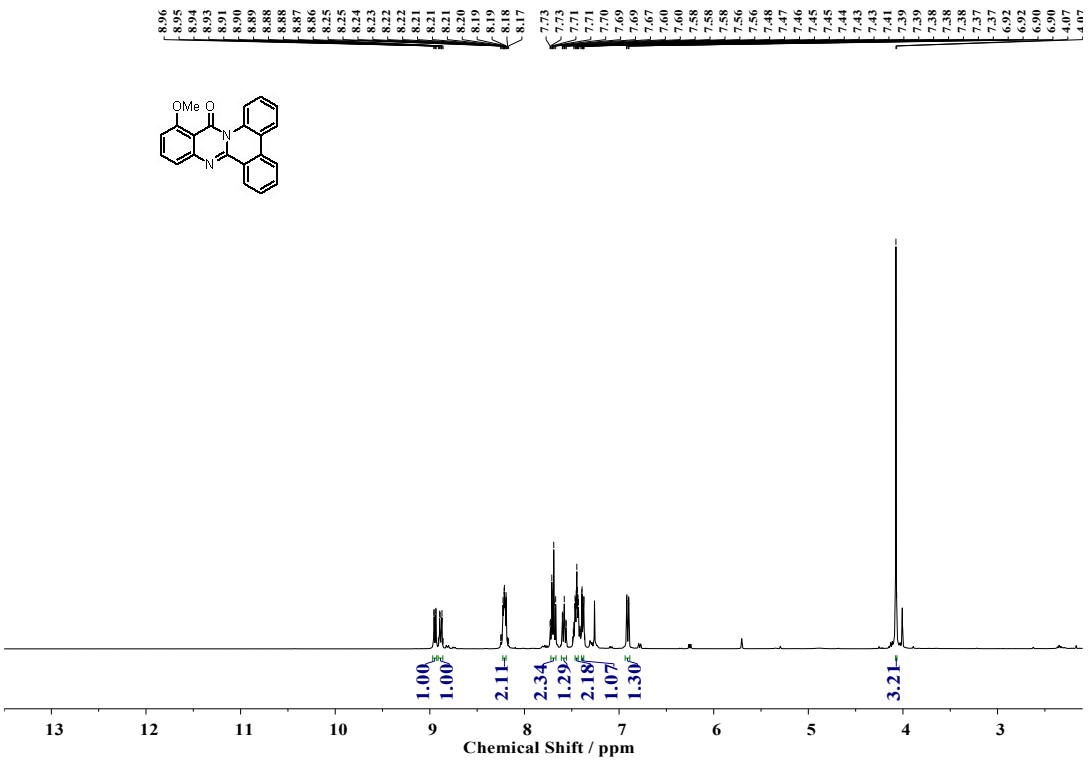


**Fig. S12** $^1H$ NMR (400 MHz, $CDCl_3$) of the compound **3b**.

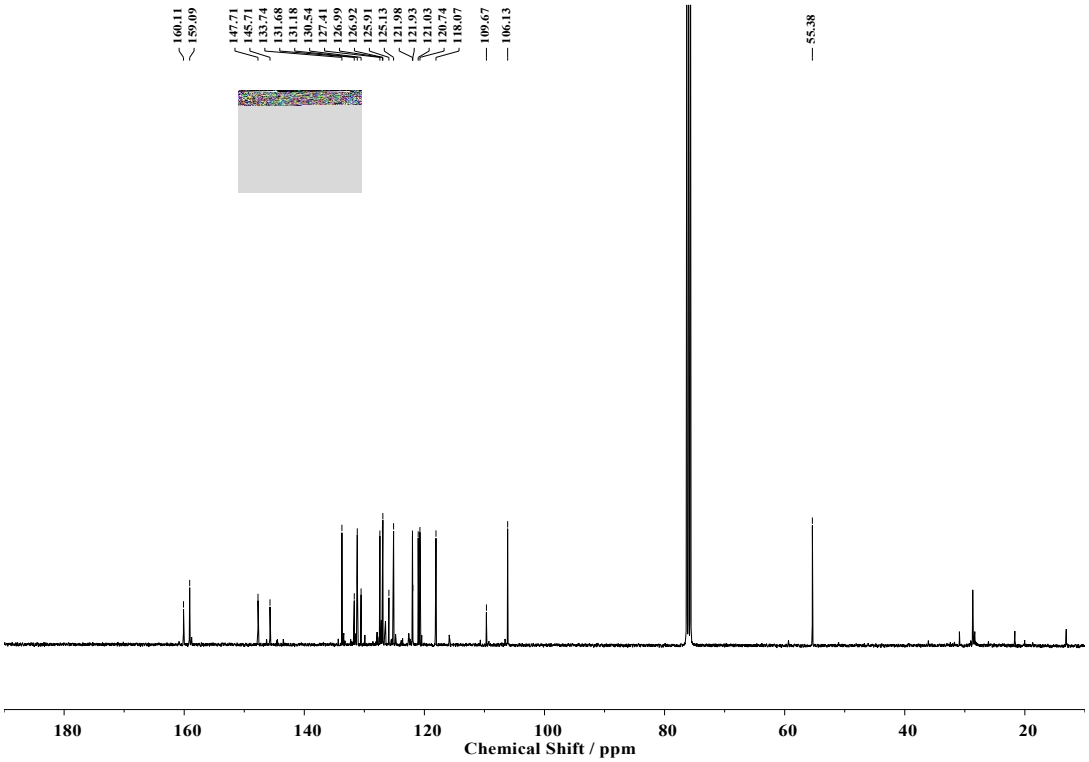


**Fig. S13** $^{13}C$ NMR (100 MHz, $CDCl_3$) of the compound **3b**.

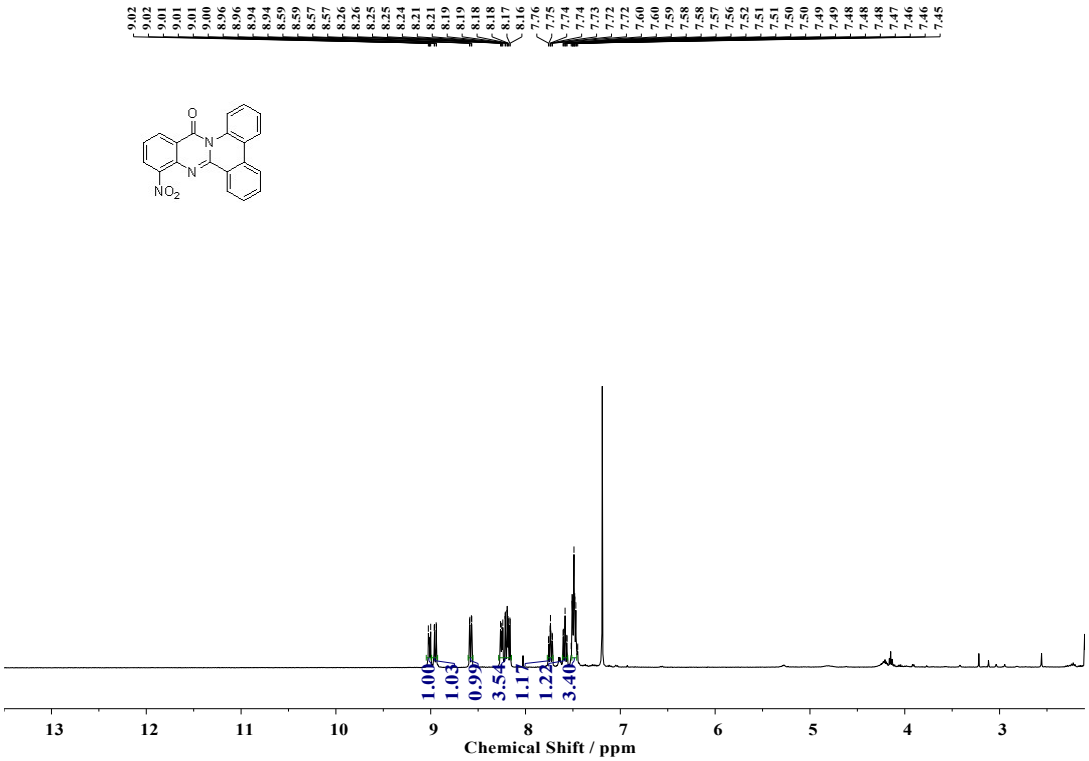


**Fig. S14** $^{1}H$ NMR (400 MHz, $CDCl_3$) of the compound **3f**.

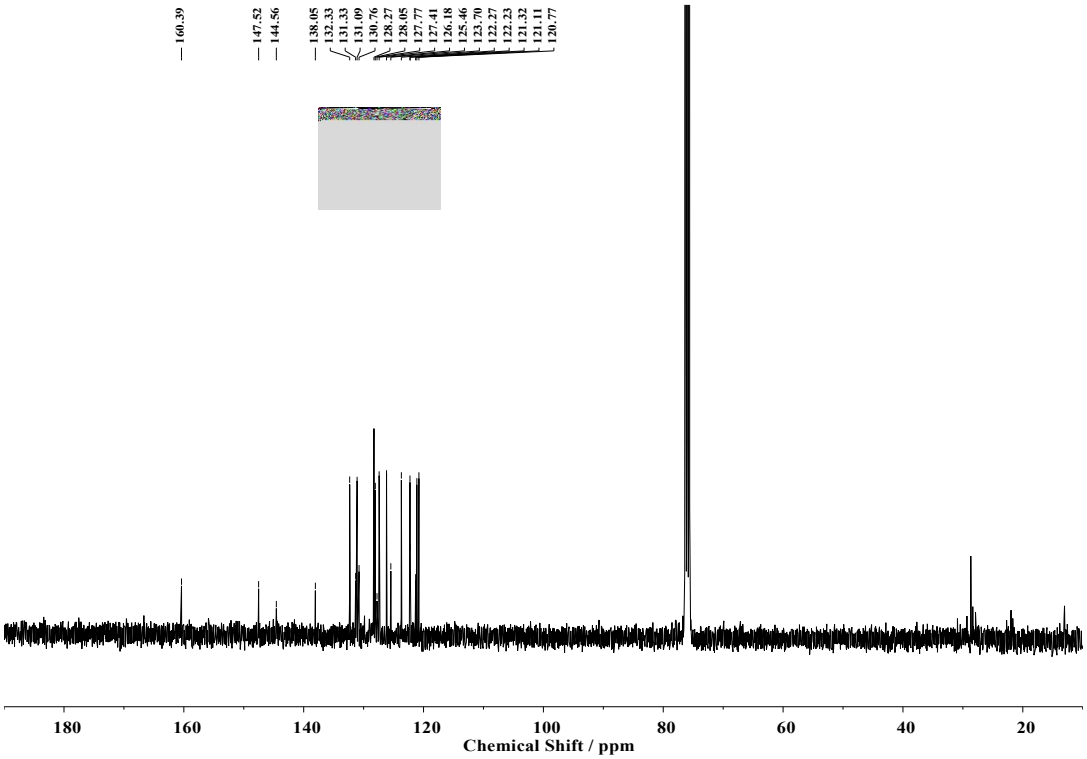


**Fig. S15** $^{13}C$ NMR (100 MHz, $CDCl_3$) of the compound **3f**.

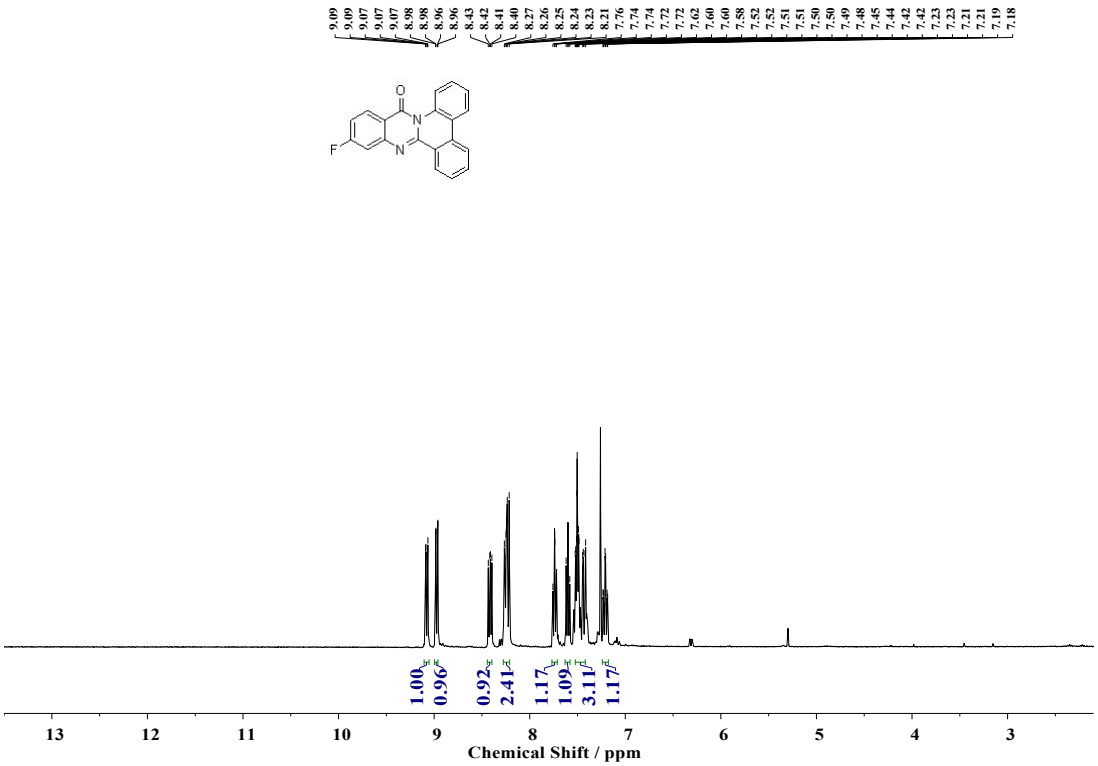


**Fig. S16** $^{1}H$ NMR (400 MHz, $CDCl_3$) of the compound **3g**.

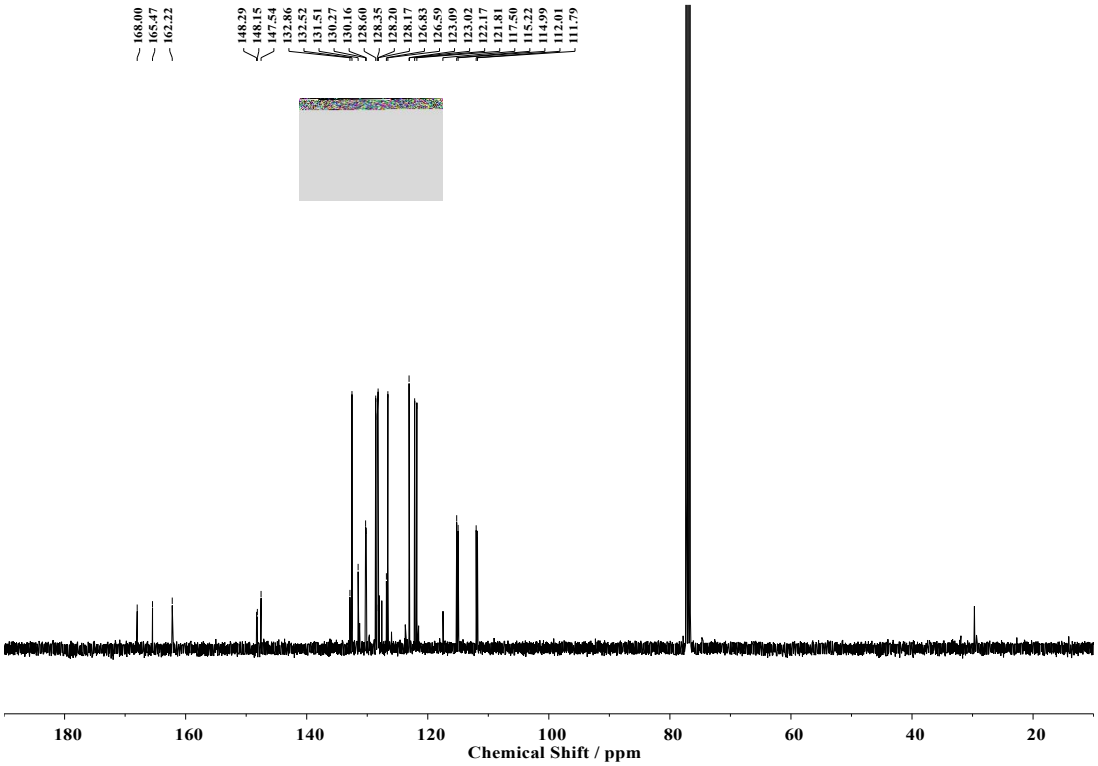


**Fig. S17** $^{13}C$ NMR (100 MHz, $CDCl_3$) of the compound **3g**.

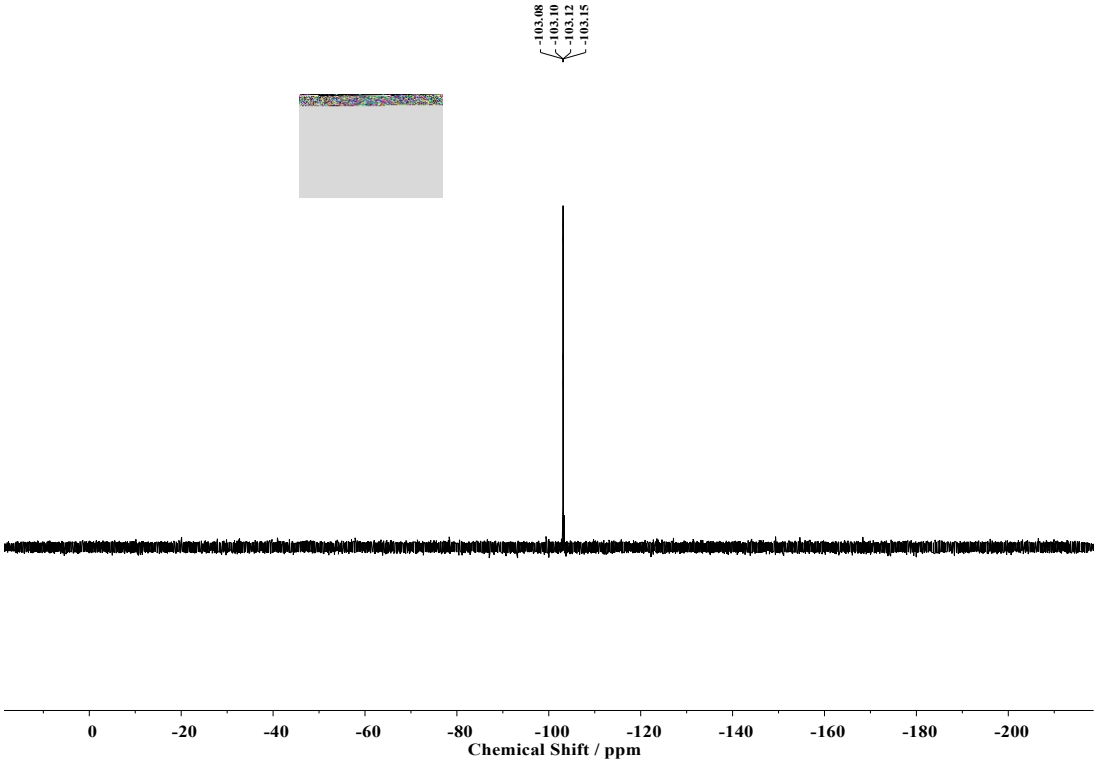


**Fig. S18** $^{19}F$ NMR (376 MHz, $CDCl_3$) of the compound **3g**.

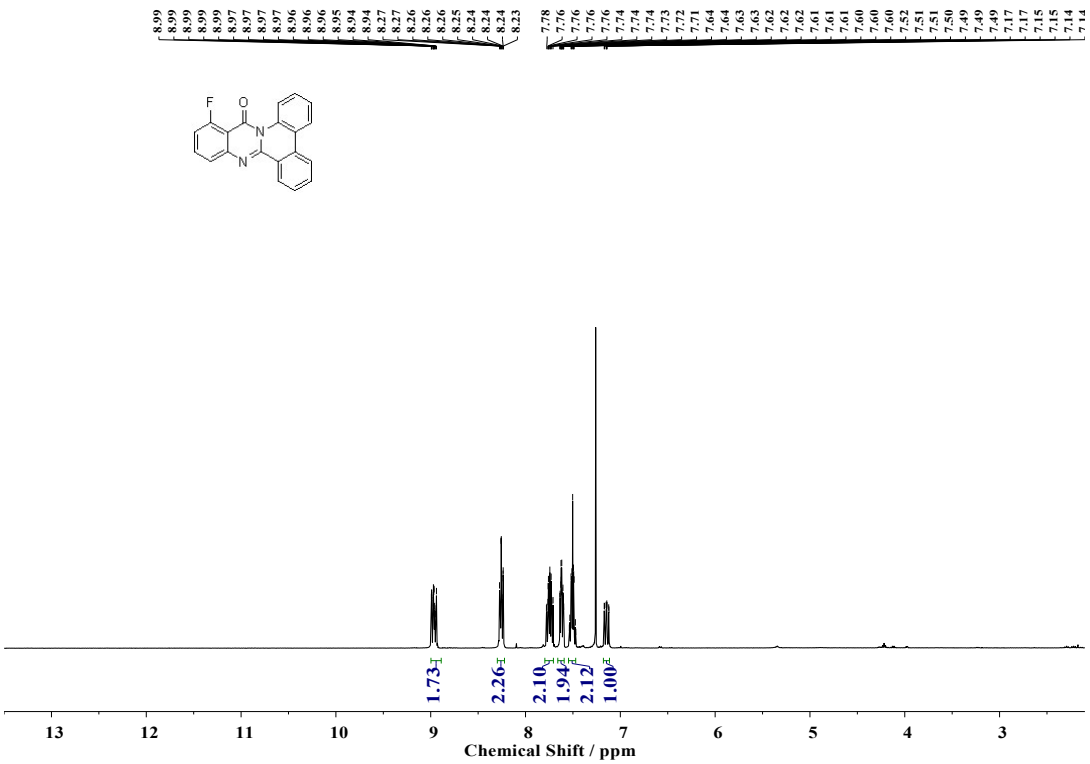


**Fig. S19** $^{1}H$ NMR (400 MHz, $CDCl_3$) of the compound **3i**.

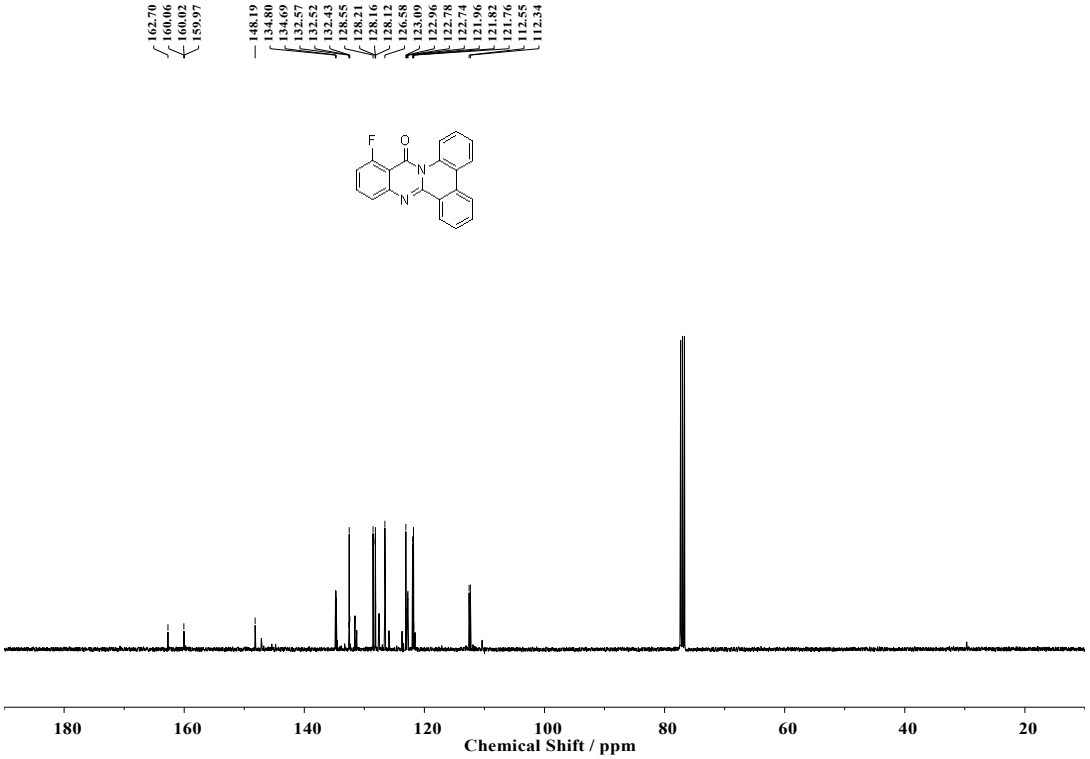


**Fig. S20** $^{13}C$ NMR (100 MHz, $CDCl_3$) of the compound **3i**.

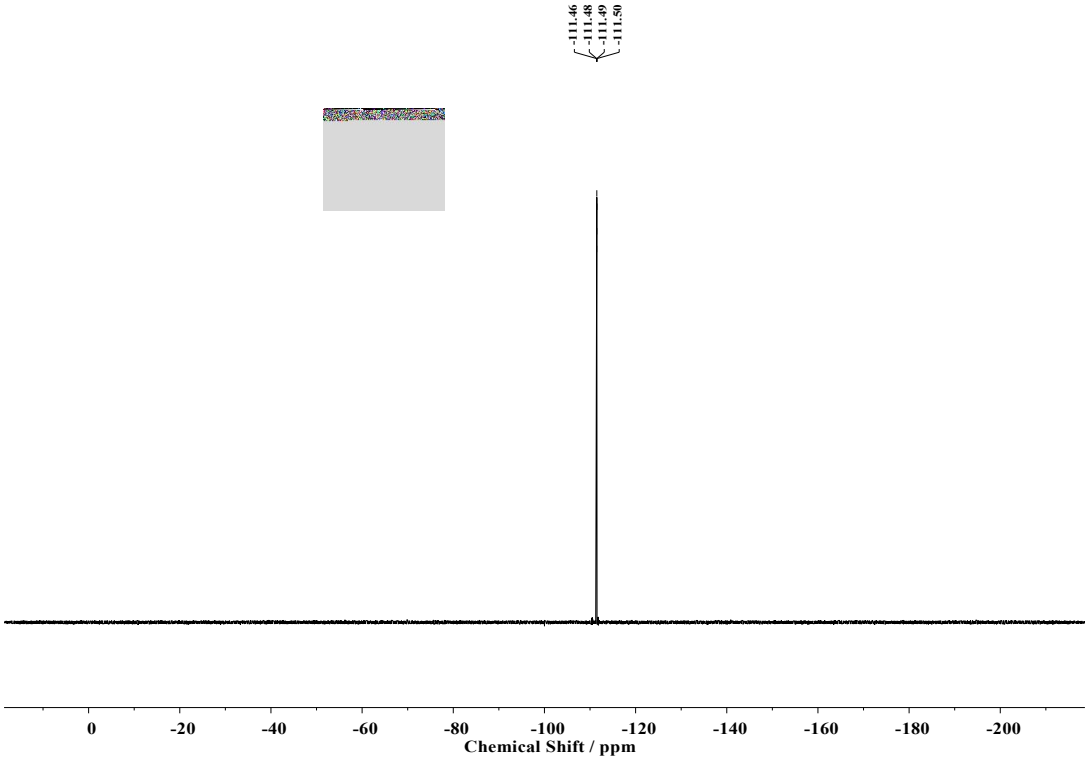


**Fig. S21** $^{19}F$ NMR (376 MHz, $CDCl_3$) of the compound **3i**.

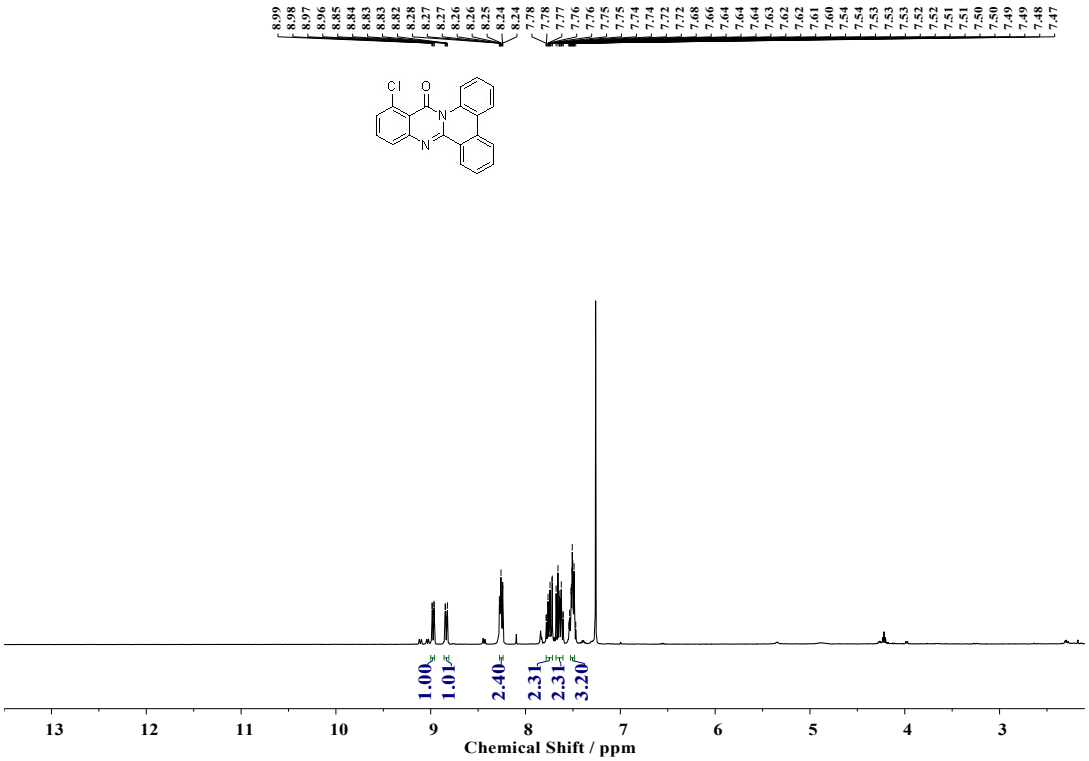


**Fig. S22** $^{1}H$ NMR (400 MHz, $CDCl_3$) of the compound **3k**.

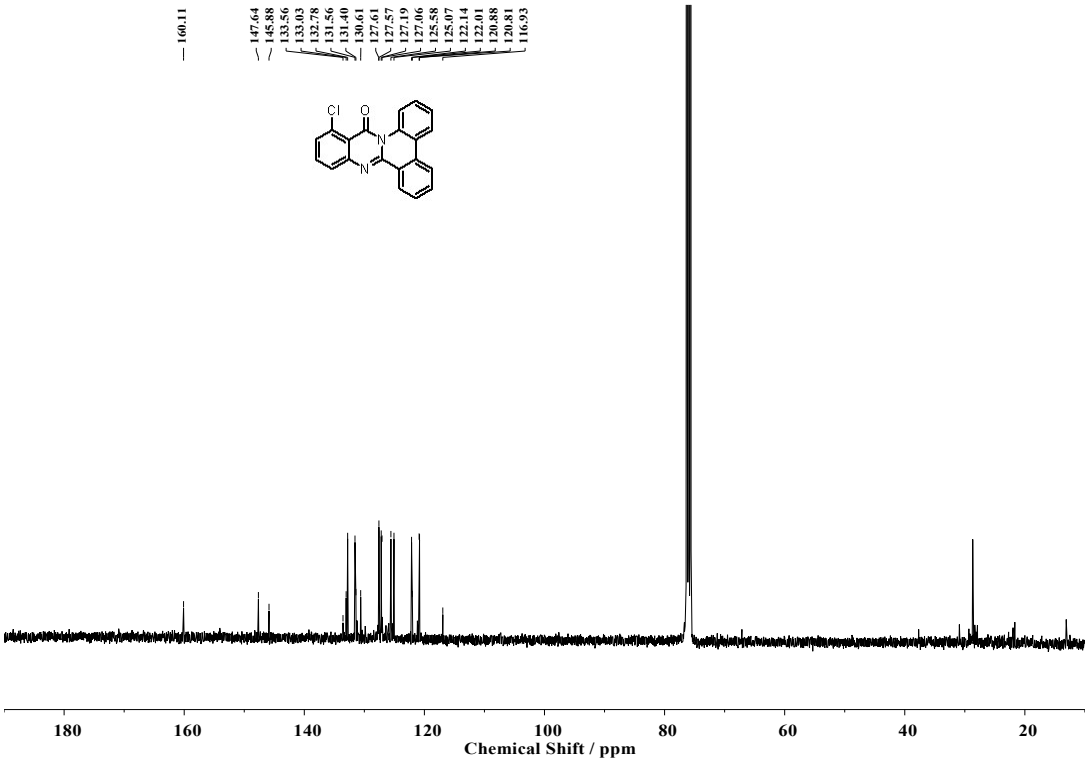


**Fig. S23** $^{13}C$ NMR (100 MHz, $CDCl_3$) of the compound **3k**.

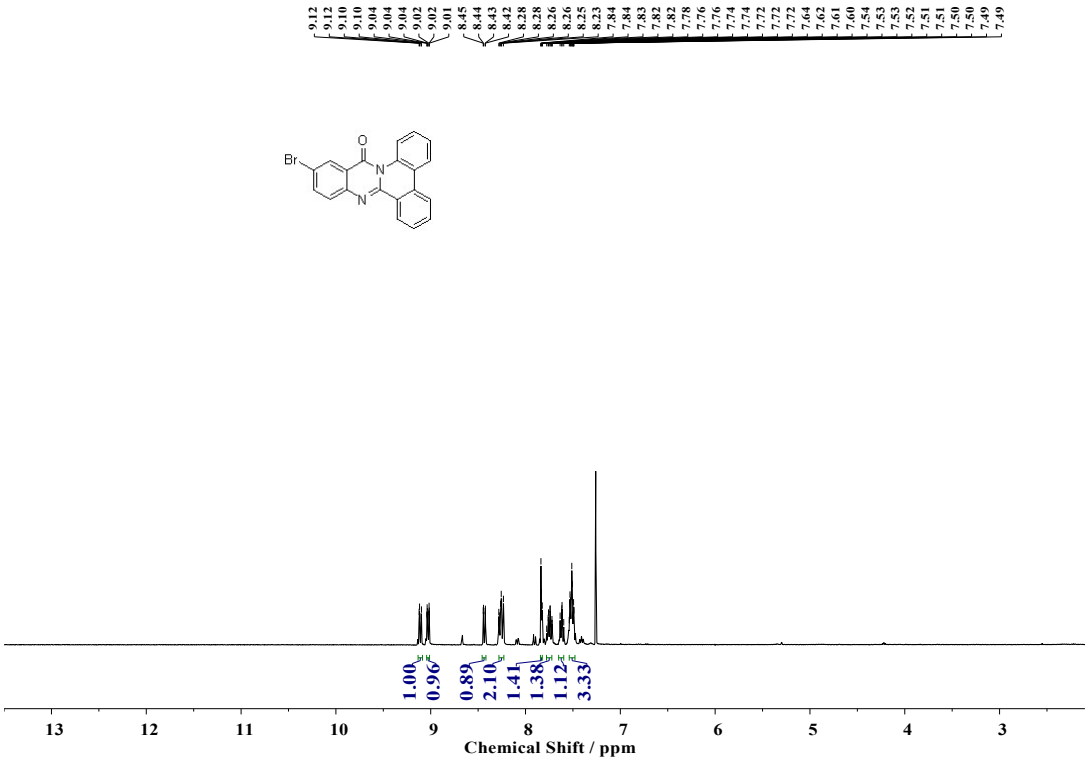


**Fig. S24** $^{1}H$ NMR (400 MHz, $CDCl_3$) of the compound **3m**.

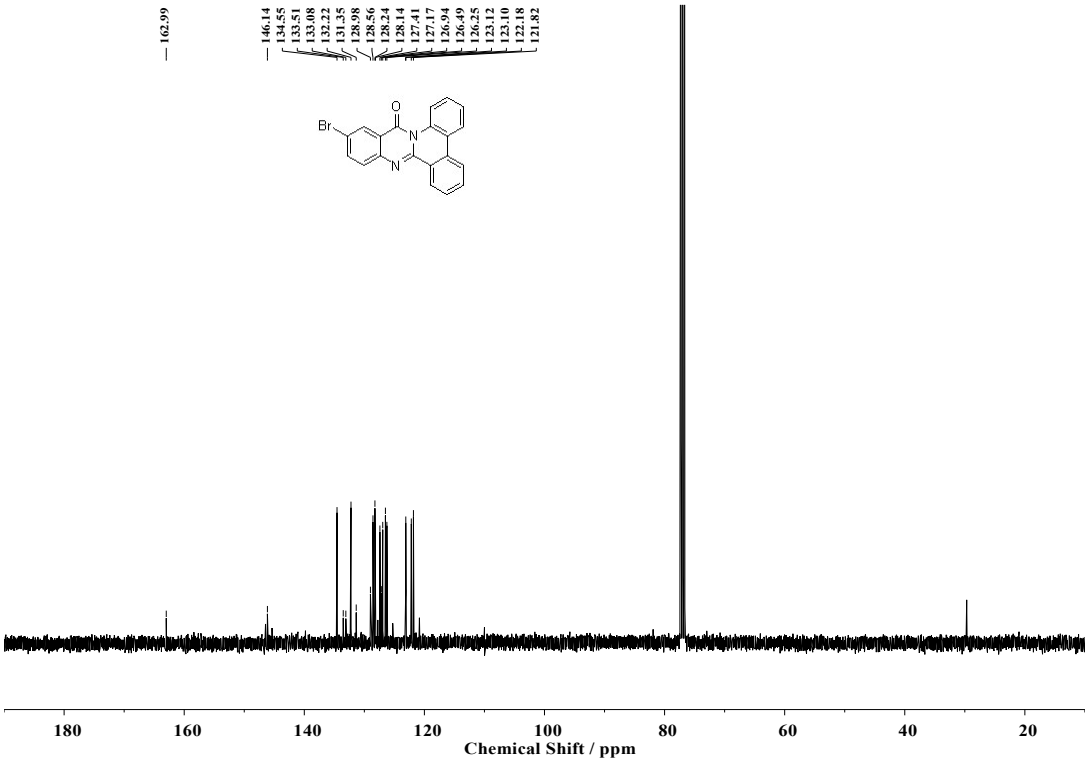


**Fig. S25** $^{13}C$ NMR (100 MHz, $CDCl_3$) of the compound **3m**.

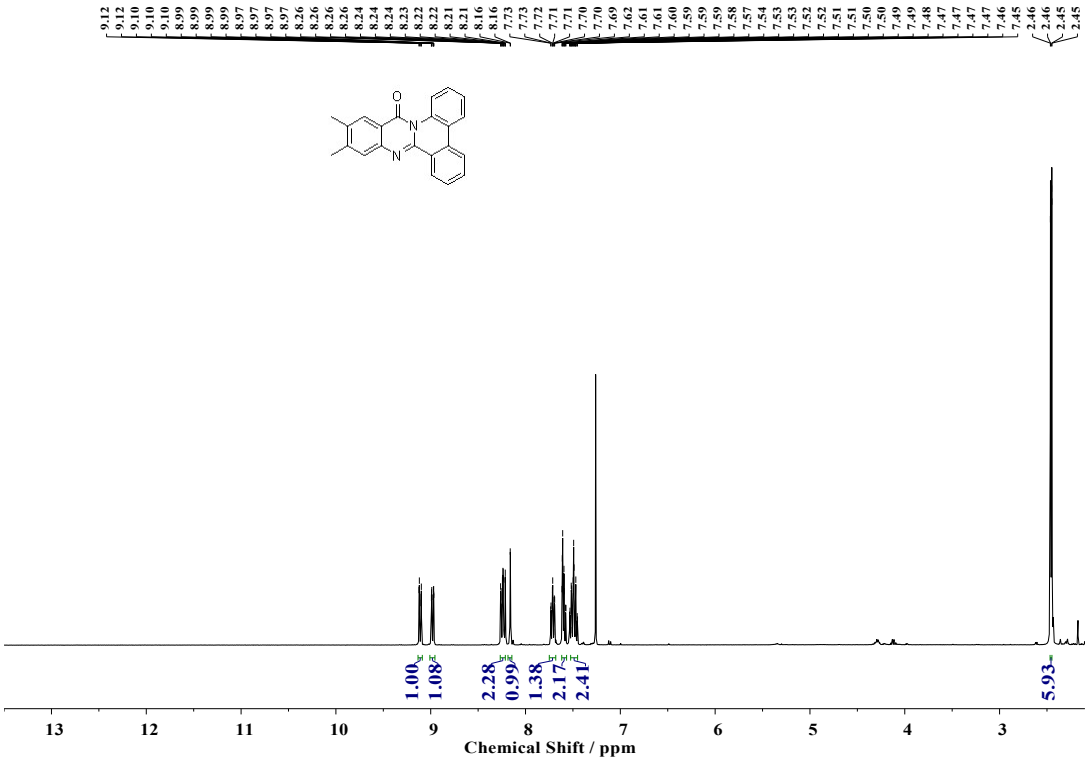


**Fig. S26** $^{1}H$ NMR (400 MHz, $CDCl_3$) of the compound **3n**.

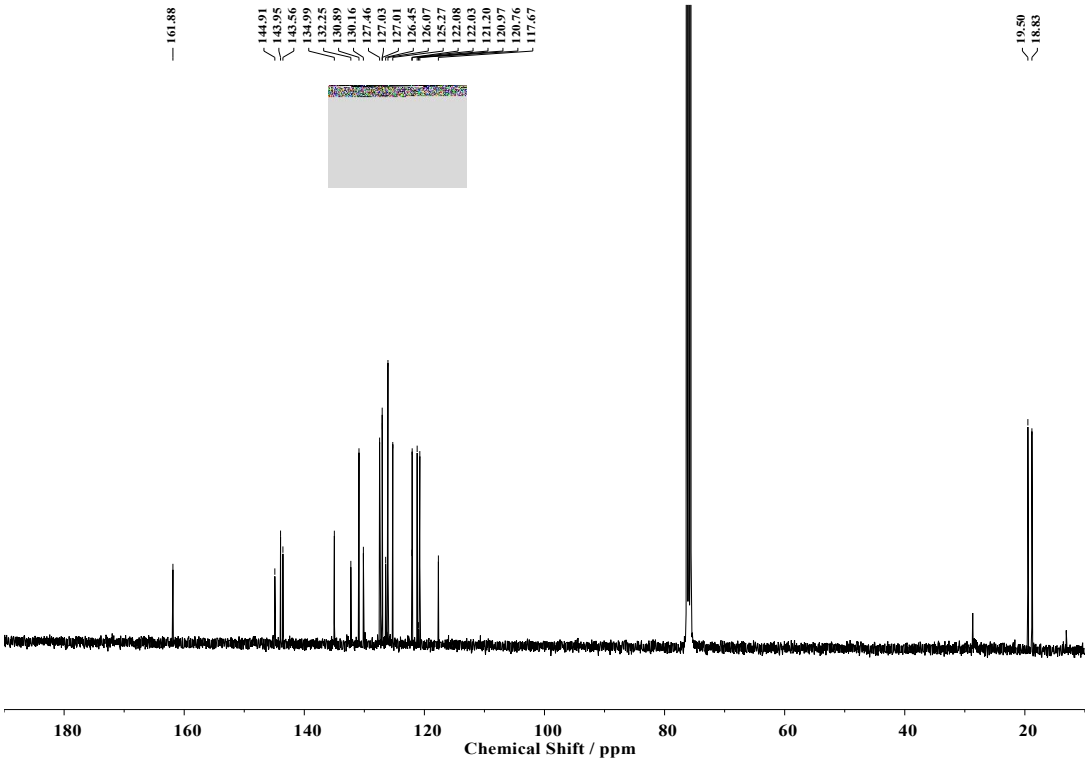


**Fig. S27** $^{13}C$ NMR (100 MHz, $CDCl_3$) of the compound **3n**.

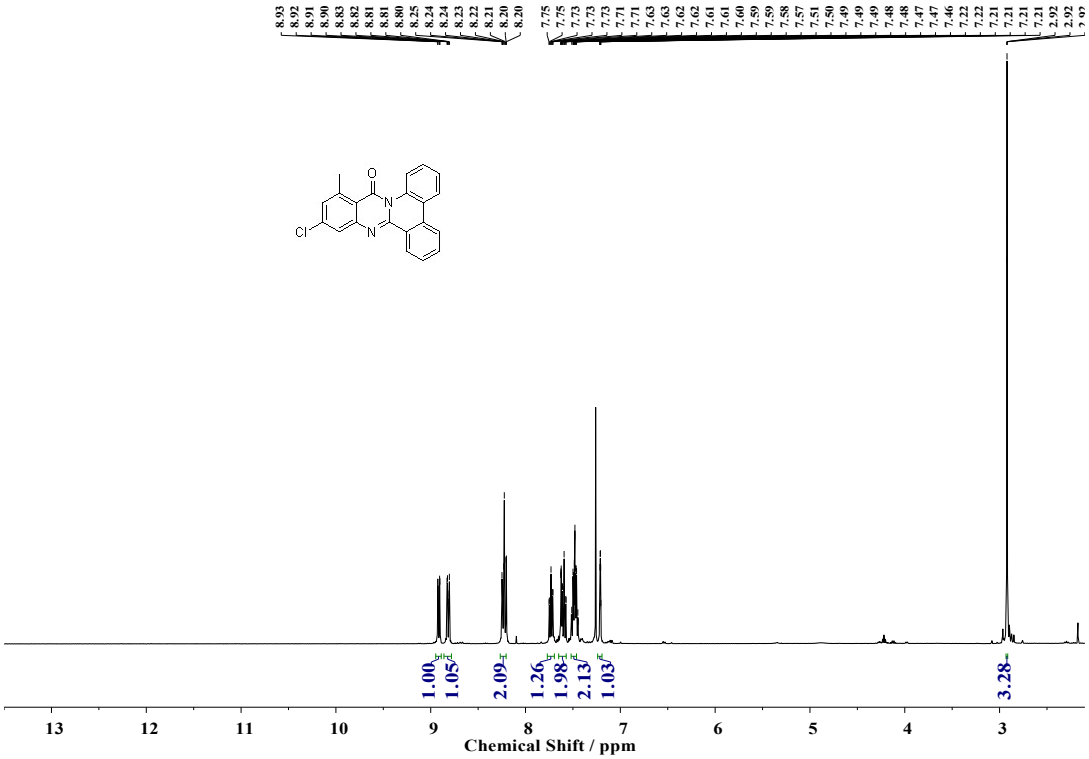


**Fig. S28** $^{1}H$ NMR (400 MHz, $CDCl_3$) of the compound **3o**.

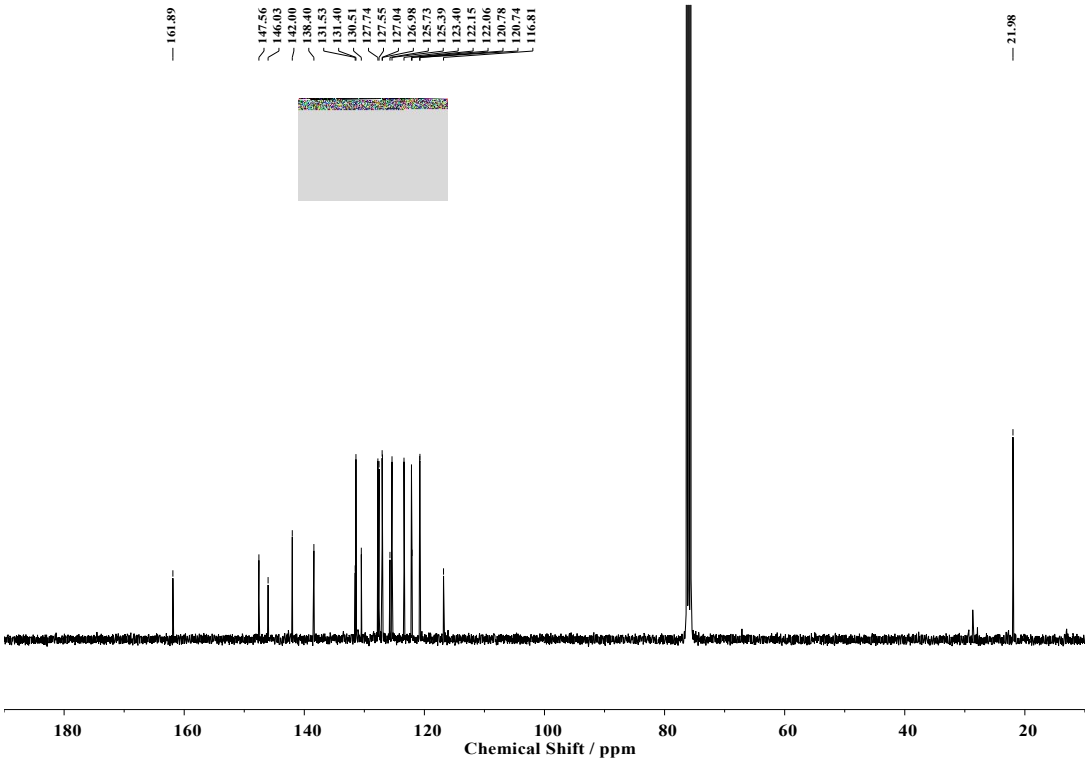


**Fig. S29** $^{13}C$ NMR (100 MHz, $CDCl_3$) of the compound **3o**.

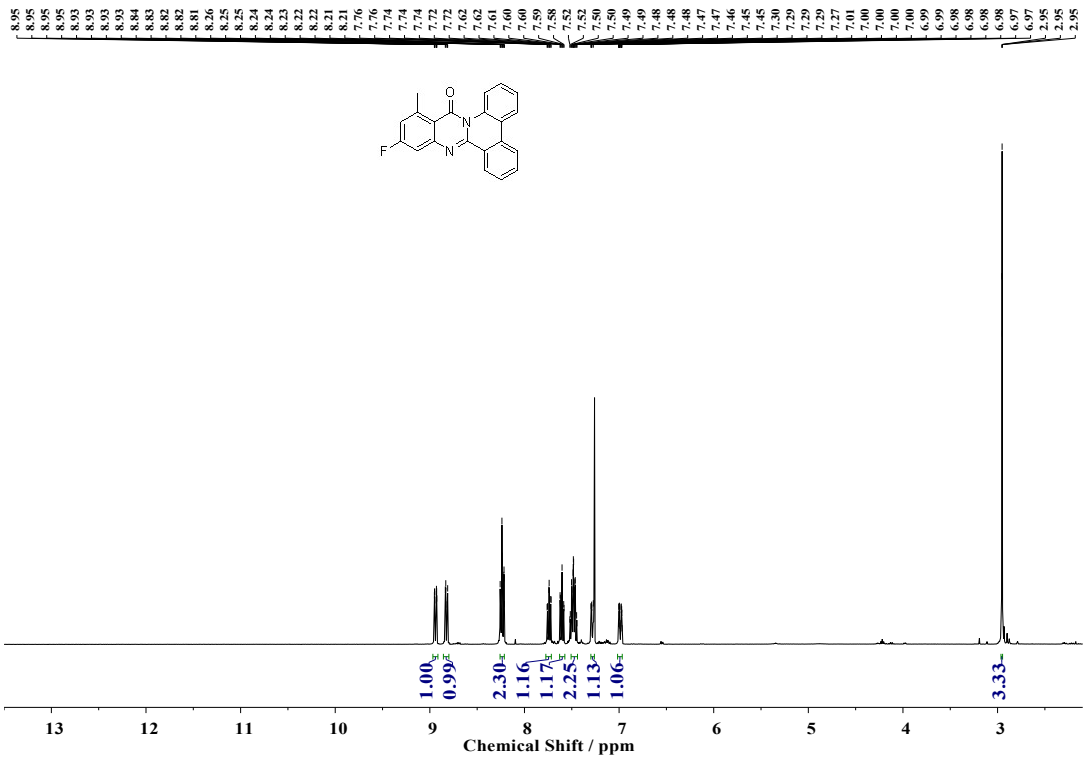


**Fig. S30** $^{1}H$ NMR (400 MHz, $CDCl_3$) of the compound **3p**.

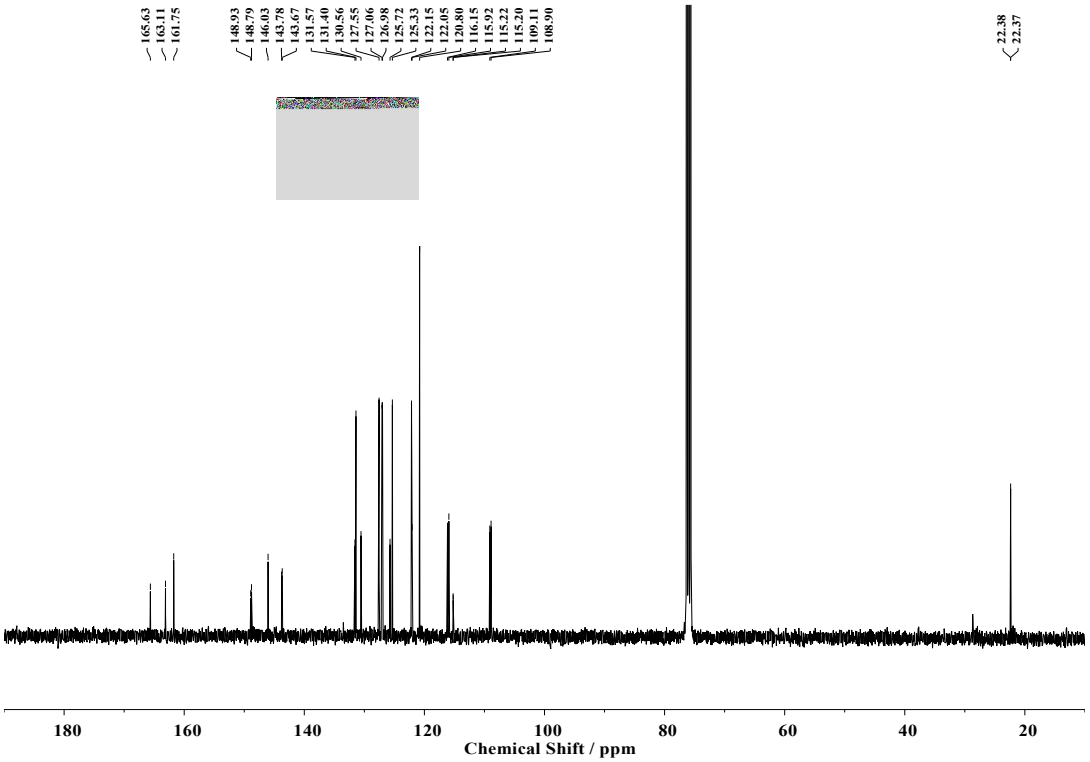


**Fig. S31** $^{13}C$ NMR (100 MHz, $CDCl_3$) of the compound **3p**.

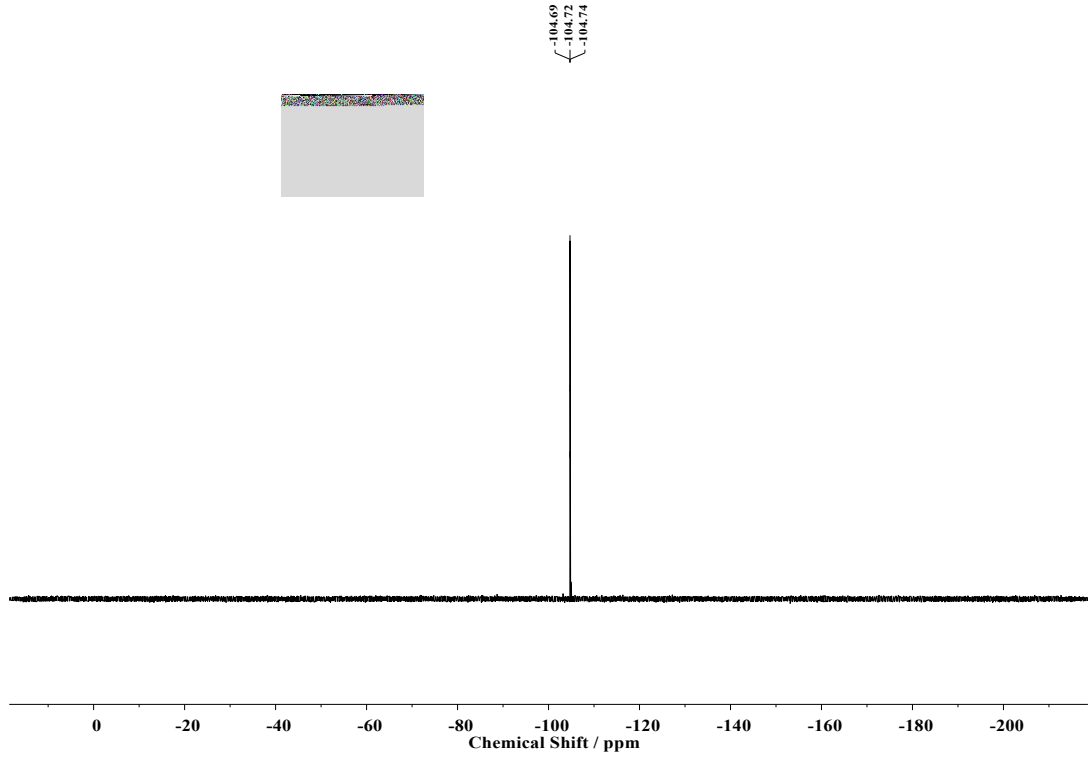


**Fig. S32** $^{13}F$ NMR (376 MHz, $CDCl_3$) of the compound **3p**.